INSTITUTO POLITÉCNICO DE BRAGANÇA
Escola Superior de Tecnologia e Gestão

Numerical Analysis of Wooden Slabs with Perforations Under Fire Conditions

Djaafer Haddad

Final Thesis Report Presented to:

Escola Superior de Tecnologia e Gestão

Instituto Politécnico de Bragança

Thesis submitted to fulfil the requirements of Ms.C degree in:

Construction Engineering

Supervised by:

Professor Elza Maria Morais Fonseca

Professor Belkacem Lamri

July 2016

Acknowledgements

At the end of this work, I would like to express my deep gratitude and my sincere thanks for “My Family” to their tender encouragement and their great sacrifices, they have been able to create the climate affectionate and conducive to the continuation of my studies.

My profound thanks go to my coordinators Pof. Elza Fonseca, and Prof. Belkacem Lamri, for their helps and advices given in my work and their interested to solve problems and find solutions to move forward.

Also I would like to thank all my friends, for supports and encouragement, specially Nabil.

Finally, my thanks go to everyone who contributed in any way to the development of this work.

Numerical Analysis of Wooden Slabs with Perforations under Fire Conditions

By:

Djaafer Haddad

Thesis submitted to fulfil the requirements of Ms.C degree in:

Construction Engineering

Supervised by:

Prof. Elza Maria Morais Fonseca

Prof. Belkacem Lamri

Abstract:

Wood is considered an ideal solution for floors and roofs building construction, due the mechanical and thermal properties, associated with acoustic conditions. These constructions have good sound absorption, heat insulation and relevant architectonic characteristics. They are used in many civil applications: concert and conference halls, auditoriums, ceilings, walls… However, the high vulnerability of wooden elements submitted to fire conditions requires the evaluation of its structural behaviour with accuracy.

The main objective of this work is to present a numerical model to assess the fire resistance of wooden cellular slabs with different perforations. Also the thermal behaviour of the wooden slabs will be compared considering different material insulation, with different sizes, inside the cavities.

A transient thermal analysis with nonlinear material behaviour will be solved using ANSYS© program. This study allows to verify the fire resistance, the temperature evolution and the char-layer, throughout a wooden cellular slab with perforations and considering the insulation effect inside the cavities.

Keywords: perforated wooden slab, insulation, fire, numerical study.

Análise numérica de lajes em madeira com perfurações em situação de incêndio

Djaafer Haddad

Dissertação para obtenção do grau de Mestre em:

Engenharia da Construção

Realização sobre a supervisão de:

Prof. Doutora Elza Maria Morais Fonseca

Prof. Doutor Belkacem Lamri

Resumo

A madeira é um material considerado como uma solução ideal para pisos e tetos em construção de edifícios, devido às suas propriedades mecânicas e térmicas, associada a boas condições acústicas. Este tipo de construções permite uma boa absorção sonora, isolamento térmico, com características arquitetónicas relevantes. As aplicações em construção são variadas: salas de conferência ou concerto, auditórios, tetos, paredes… Todavia, a alta vulnerabilidade dos elementos de madeira submetidos a condições de incêndio, requer a avaliação de seu comportamento estrutural com precisão.

O principal objetivo deste trabalho é apresentar um modelo numérico para avaliar a resistência ao fogo das lajes celulares de madeira com diferentes perfurações. Também o comportamento térmico de lajes de madeira serão comparadas considerando diferentes materiais de isolamento, com placas de espessura diferente no interior das cavidades.

Será utilizado o programa ANSYS© para a análise térmica e transiente com comportamento do material não-linear. Este estudo permite verificar a resistência ao fogo, a evolução da temperatura e a determinação da velocidade de carbonização, para as lajes celulares de madeira com perfurações, considerando ainda o efeito de isolamento no interior das cavidades.

Palavras-chave: laje de madeira perfurada, isolamento, fogo, estudo numérico

Index

Index of Figures

Index of Tables

Chapter 1

Introduction

1 Introduction

The problem of the fire resistance in wooden elements is analysed from the behaviour that the material presents when is exposed to fire action. Fire resistance relates to the period for which an element will resist to a flame passage, remains free from collapse and insulate against an excessive temperature rise of the unexposed face. Different fundamental phenomena need to be evaluated: combustion, heat transfer and wood properties degradation with temperature dependence, [1].

In this work different wooden cellular slabs are considered for study with typical applications in construction engineering, as auditoriums, offices, restaurants, concert halls, schools, hotels, gymnasiums, etc. Also they are typical panels applied in building structures with a rustic and decorative look. The combination between the wood materials and other acoustic material layers offers aesthetics and sound absorption effect. The perforations in these slabs are common and available in different patterns and sizes. Fire experimental tests in different wooden surfaces were performed by Frangi et al. [2], presenting some results of the fire tests and show a simplified calculation model for the burning rate compared with the test results. Two different charring phases were taken into account for this model. The results showed that fire penetration into the cavities of the hollows elements can be prevented, if the perforated acoustic layer and the sound absorbers placed behind it are sufficiently thick. Before and after the perforated acoustic layer is completely charred, and the fire tests clearly showed that the charring rate during the first phase is mainly influenced by the size and the position of the perforations, as well as, the thickness of the perforated acoustic layer.

Wood is a thermally degradable and combustible material. Wood when subjected to fire produces a surrounding charring depth layer, with no mechanical resistance, resulting a reduced cross-section. Several researchers have presented experimental models and analytical methods to calculate the physical degradation of wood due to high temperatures. In 2004 Jassens [3] presented a new model to calculate the charring rate and temperature distribution to predict the thermal degradation, referred by the acronym CROW (Charring Rate of Wood), and take into account the factors that affect the thermal degradations of wood (dry density; moisture content; lignin content; char contraction, with some adjustment for moisture effects). The CROW model appears in reasonable agreement with the measurements, and it is useful to predict performance of wood members exposed under thermal conditions.

The charring rate is strongly affected by the material density and it has been studied by different researchers. In 2008 Frangi et al [4], present research of a charring model based on an extensive finite element thermal analysis, for timber frame floor assemblies with void cavities. The results showed that the charring model takes into account the influence of high temperature after failure of the fire protective claddings, as well as, the heat flux superposition on the charring rate of the timber beams exposed to fire on three sides.

In 2003 Frangi and Fontana M. [5] were also worked on the fire behaviour of timber slabs, made of hollow core elements and of timber-concrete composite slabs contributed to the experimental database of charring and temperature measurements of wood members exposed to fire. The results showed simplified methods based on a constant charring rate to calculate the fire resistance of wood elements. They are confirmed by the fire tests with different timber members exposed to the standard ISO fire [6] of 30-110[min], also the use of a simplified method for the fire resistance of load bearing wood sections should therefore only be used up to a residual cross-section of 40-60[min]. The temperature profiles through wood members exposed to fire depend on the duration of fire exposure.

Also in 2010 Cachim P.B and Franssen J.M, [7] worked with two calculations methods from EC5. They used simplified and advanced methods for the calculation of fire resistance in timber structures. The methods are regarding the calculation of the char depth and residual cross section strength. They produced also finite element simulations, performed using the code SAFIR, the numerical results indicate that both models have some limitations. According their results some proposals to overcome the inconsistencies, as well as, to extend their applicability, namely an expression to calculate the charring rate, as a function of density and moisture content.

In 2009 Fonseca E.M.M and Barreira L.M.S, [8], [9] propose an experimental and a numerical method for charring rate determination in pine wood. Different pine sections were tested and submitted to high temperatures using a heating power unit based on electrical resistances. The temperature results were measured through wood profile during time heating exposure and a finite element analysis with ANSYS© program was used for charring layer determination. The obtained results were compared with experimental results from pine wood. The results showed an agreement between the two alternative methods.

In perforated cellular wooden slabs, the size of perforations facilitates and increases the heat flow and flames penetration over the slab. An insulation material in combination with other building materials allow to reduce the heat transfer inside and outside of the element. There are many kinds of insulating materials, each of which has its own set of advantages and disadvantages, and none of which is the perfect solution. The best insulation materials should have the lowest thermal conductivity, in order to reduce the total coefficient of heat transmission. The insulation material should be rated as non-flammable and non-explosive. In the event that the insulation material burns, the products of combustion should not introduce toxic hazards. The main question is to choose the correct thermal insulation material which helps to satisfy building requirements as a mostly energy and cost efficient.

In 2013 Fonseca E.M.M., et al [10] proposed a numerical model to assess the fire safety of wooden slabs with rectangular perforations on a ceiling. An internal fibreboard insulation material was added inside cavities. Finite element program was used for nonlinear material in transient thermal analysis to allow verifying the temperature evolution, the char-layer throughout the slab and verifying the influence of the use of a fibre board. The results showed that the type and the size of perforations can limit the use of these constructive elements in terms of fire resistance. Also, the use of insulation material limits the heat penetration and the charring rate is lower. As a conclusion, the constructive elements should be chosen before, to prevent and delay the fire damage effect.

In the same year 2013 Fonseca E.M.M et al. [11] developed a numerical model to assess the fire behaviour of cellular wood slabs with different drillings. A transient thermal analysis with nonlinear material behaviour was solved with ANSYS© program. The main goal was to present a numerical model based on a constructive solution proposed by Frangi and Fontana 2004, [12] to calibrate the numerical results. The results for charring depth indicate that the numerical method reveals good performance when compared with the experimental model. In case of fire exposure, the type and size of perforations should be chosen before, allowing that the slab could remain in service during more time.

In 2015 David C., et al., [13] present a 3D constructive models for different experimental tests at real scale in laboratory, representing four cellular wooden slabs. These slabs were tested in a fire resistance furnace with the objective to predict the evolution of the charring layer during a fire scenario in a constructive solution with circular perforations.

Additional work produced in 2015 David C., et al., namely with Meireles [14] presenting a 3D constructive models for experimental tests in laboratory, representing cellular wooden slabs but now with different circular perforations. These slabs were tested in the same fire resistance furnace, as the previous, to predict the evolution of the temperature and the charring layer in constructive solutions.

In the present work, the main goal is the use of an advanced calculation method for determining the charring depth, the profiles and the temperature distribution through the construction elements during a fire scenario. A finite element program (ANSYS©) will be used for transient and nonlinear material thermal analysis. This work describes the basic idea of a 2D and 3D numerical model, to predict the time temperature history and the residual cross-section identification in wooden cellular slabs with and without perforations. The initial validation of the numerical model will be obtained using the experimental tests from David and Meireles [13], [14]. In addition, different constructive solutions will be numerically analysed, and insulation material will be added inside the cellular cavities to determine the influence on time-temperature history. Also the cavities with insulation will be fulfil with internal air. The numerical models combine different materials, as temperature dependent and constant values. The main results of the numerical analysis are presented and the proposed 2D models are compared with 3D models to represent more realistic situation. The results enlarge the knowledge of the fire behaviour of different insulation materials applied in wooden slabs, and complete others investigations developed by the supervisors of this work.

1.1 Objectives

In this work, the main objective is to perform numerical tests in different wooden slabs with perforations and also using insulation materials, to predict the fire resistance time and the charring rate evolution during a fire scenario. Different 2D (two dimensional) models will be tested numerically, representing cross-sections of real models previous tested and submitted to a real fire [10-11], [13-14]. At this stage, it is intended to verify the accordance between the results, using reduced and simplified computational models. Also the calculation of charring layer will be compared with the design value proposed by the Eurocode 5 part 1.2 [15]. In

addition, all two dimensional models will be reproduced, but with different insulation material to verify the influence in fire resistance. At the last step, 3D (three dimensional) numerical models will be produced to study wooden slabs with perforations. In all numerical simulations, appropriate material properties and boundary conditions will be used to predict the real fire effect.

The main goal of this work is to present different constructive numerical solutions of wooden slabs with rectangular or circular perforations, with or without insulation material, to study the fire resistance in such way that contributes for a safe design. The subject of this work is an ongoing project, according to others investigations produced and tested in the laboratory of the Polytechnic Institute of Bragança with typical wooden slabs submitted to experimental tests, [10-11], [13-14].

During all steps of this work different programs for calculation, drawing and analysis were used. The software used in this work are the following: Excel, Autocad and ANSYS©.

1.2 Summary of the chapters

More six additional chapters will be presented in this report with all described work and steps to concretize the final master thesis.

In **Chapter 2** of this work, a description of the heat transfer mechanisms by conduction, convection and radiation, will be presented. Also, parametric curves defined by Eurocode 1 part 1.2 [16], ASTM E119, [17] and the standard curve of natural fire, which characterizes the time temperature evolution, are presented.

Chapter 3 explains the thermal behaviour of materials and presents the thermal properties of wood and insulations material used in this study (MDF, Medium Density Fibreboard and RW, Mineral Wool), namely the thermal conductivity, specific heat and the specific mass.

In **Chapter 4** a description of the finite element method (FEM) used in this work with the equations used for heat transfer and general boundary conditions will be explained. Also this chapter permits to increase the knowledge about different equations used in FEM to solve

problems, describes the thermal diffusivity equation and presents the shape functions of the finite element for 2D and 3D meshes.

In **Chapter 5** description of different 2D and 3D models is exposed based in the dimensions of a constructive real solution, for results comparison. A transient thermal analysis with nonlinear material behaviour will be developed using ANSYS© program. The char layer formation through time in wood slabs submitted to fire will be calculated. All boundary conditions are well defined and the type of results (profile of temperatures, char layer and charring rate) are presented in all slabs in study.

The last two chapters, chapter 5 and chapter 6, are related with the ‘’Conclusions and Future Work’’, and the ‘’References’’ that supports the state of the art of this report.

Chapter 2

Fire Action

2 Fire Action

2.1 Heat Transfer

The basic development of the heat transfer is needed to calculate the char layer evolution in wood materials when submitted to fire. In general, the heat transfer is based on the principle of conservation of energy. This principle shows that the amount of energy used must be equal to the sum of the energy leaving and stored in the system. Applying the conservation principle of energy to heat transfer rates, the first law of thermodynamics could be presented as follows, [18].

$$dU = dQ - dW \tag{1}$$

Where **dU** is the modification of internal energy in the system, **dQ** is the amount of heat added to the system; **dW** is the amount of work done by the first law of thermodynamics.

This law means that if no work is done by the system, the change in internal energy must equal the heat change in the system, [18]. The three components were generally implied in the heat transfer are: conduction, convection and radiation. According the definition, conduction is the mechanism for heat transfer through solid materials, convection is the heat transfer by the movement of fluids, either gases or liquids and radiation is the transfer of energy by electromagnetic waves, [18].

2.2 Modes of Heat Transfer

The heat transfer knowledge in engineering consists of the evaluation of three modes with specific conditions, properties and geometries, and with further application than that usually used to design and performance analysis of heat exchangers, [19].

There are three different kinds of heat transfer which are usually referred to as heat transfer mode: conduction, convection and radiation, as shown in figure 1.

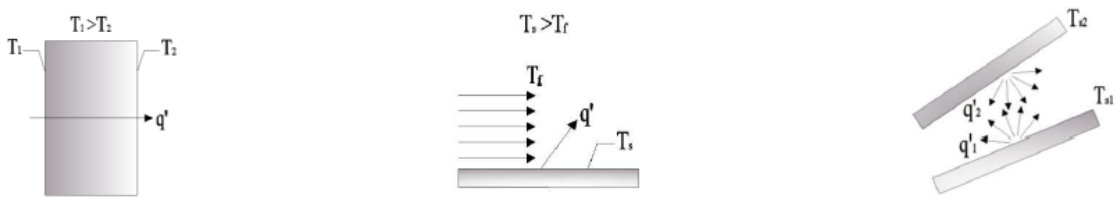

Figure 1- Conduction, convection and radiation, [20].

2.2.1 Conduction

As defined, “Conduction is the transfer of energy from more energetic particles to less energetic ones due to interaction between atomic and molecular particles”, [19]. The conductive heat transfer is schematized in figure 2.

Conduction can occur in: solid, liquid and gaz. “In solids conduction the heat transfer is due to the combination of vibrations of the molecules in a lattice and energy transport by free electrons”, [19]. Conduction is the diffusion and collision of molecules in gases and liquids during their random motion, [19].

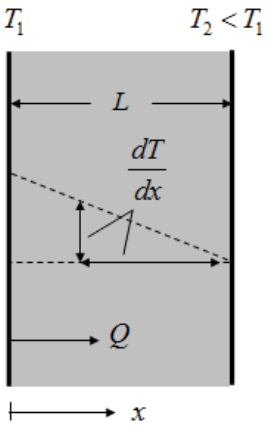

Figure 2- Conductive heat transfer, [21].

The equations 2 and 3 define the heat flow, related by Fourier's Law, as a model proposed as early as 1822, [21].

$$Q = -KA\frac{dT}{dx} \tag{2}$$

$$q = -K\frac{dT}{dx} \tag{3}$$

Considering the finite slab of material shown in Figure 2, for one-dimensional conduction the temperature gradient is given by the following equation, [21].

$$\frac{dT}{dx} = \frac{T_2 - T_1}{L} \tag{4}$$

Substituting in equations 2 and 3 the transfer law can also be written:

$$Q = kA\frac{T_1 - T_2}{L} \tag{5}$$

$$q = k\frac{T_1 - T_2}{L} \tag{6}$$

Where **A** is the area through which the heats flow, in normal to the x-direction, **Q** is the heat flow conduction in the x-direction, **q** the heat flux normal to the x-direction, **K** is the positive constant of the material thermal conductivity [W/m°C], **dT/dx** is the temperature gradient in x-direction [K/m], **T** represents the temperature [°C] and **L** represents the thickness [mm].

According to the previous equations, the variation of the thermal conductivity is related to the increase in temperature. The materials are not similar, each of which has its own set characterization. In some materials the temperature increase varies between 50 to 100 times compared to the values of the ambient temperature, such as: silver, copper and aluminium. Also there are materials which the variation of the temperature is very low, [22].

2.2.2 Convection

Convection heat transfer is a mode which consists of two mechanisms: random molecular motion which is termed diffusion or the bulk motion of a fluid carries energy from place to place. Convection takes place between a fluid in motion and a boundary surface when they meet at different temperature, [21]. Heat transfer by convection can be classified in accordance with their nature by free convection and forced convection. In forced convection, the fluid motion is driven by some external influence (artificial), [19, 21].

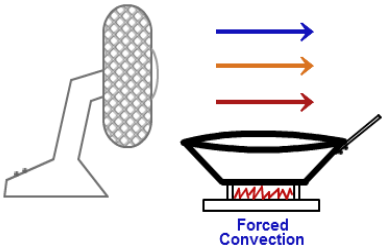

Figure 3- Forced convection, [23].

In natural or 'free' convection, flow is induced by buoyancy forces, which are caused by variations of temperature formed due to heat transfer in the fluid, [19].

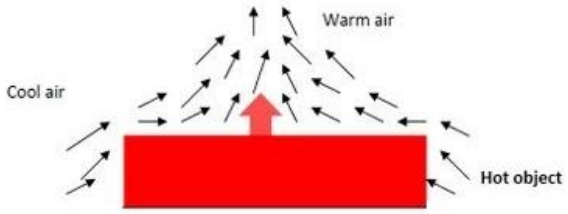

Figure 4- Natural convection, [24].

The convective heat transfers **Q**, is defined by Newton's law, [21]:

$$Q = h_c \times \left(T_s - T_f\right) \tag{7}$$

Where $\mathbf{T_s}$ is the temperature of the surface receiving or giving heat, $\mathbf{T_f}$ is the average temperature of the stream of fluid adjacent to the surface, $\mathbf{h_c}$ is the convective heat transfer coefficient which has units equal to [W/m^{2}K]. If the fluid temperature is higher, the heat flux is given by the expression, [25].

$$Q = h_c \times \left(T_f - T_s\right) \tag{8}$$

2.2.3 Radiation

Radiation is the energy transmits by all matter that has a nonzero temperature. This energy is transmitted in the form of electromagnetic waves. The propagation of electromagnetic waves changes the electronic configuration of atoms and molecules. Energy transfer due radiation is very efficient also in vacuum. It is considered as transfer phenomenon between solid surfaces, [19]. Stefan-Boltzmann law allows the calculation of the maximum rate of radiation of a blackbody or ideal radiator. The upper limit of emissive heat transfer is given by Stefan-Boltzmann law as, [19]

$$E_b = \sigma T_s^{\,4} \tag{9}$$

Where $\mathbf{E_b}$ is the emissive power of blackbody [W/m^2]; $\boldsymbol{\sigma}$ is the Stefan-Boltzmann constant equal to 5.6697×10^{-8} [W/m^{2}K^4]; $\mathbf{T_s}$ is the absolute temperature of the surface in [K]. “Heat flux emitted by real surface is less than that of blackbody at the same temperature and is given as”, [19].

$$E = \varepsilon \sigma T_s^{\,4} \tag{10}$$

Where **E** is the Emissive power of real surface [W/m^2], ε is the emissivity that depends strongly on material and finish of surface, which varies between zero and one.

2.3 Fire curves

A natural fire occurs when there is a presence of three important causes: source of heat, fuel and oxygen. The combustion happens when these three elements are mixed at a specific temperature; the natural fire curve is divided into four successive phases: ignition, initial phase, full combustion and cooling phase, [26].

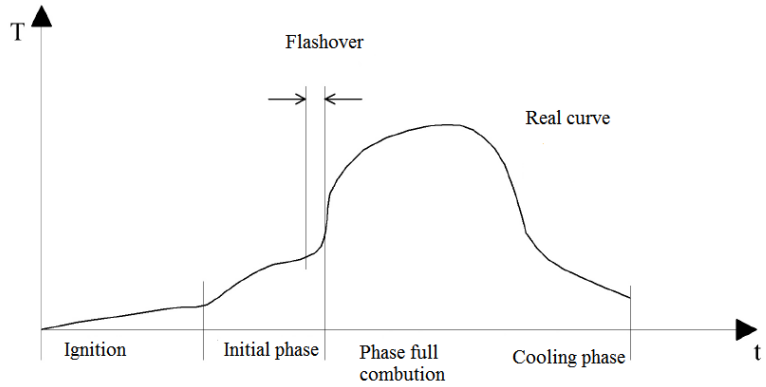

Figure 5- Fire development, [22].

In the first phase, or initial phase of ignition, the temperatures are lower and do not cause any influence on the structural behaviour of buildings. Moreover, in this phase toxic gases occurs that affects human health, [26]. The phase of the propagation, the fire could spread by radiation or by direct contact. The radiation is going to influence all combustible materials at a given moment. Than a critical phase of a fire "Flashover" happens, in which temperatures are between 450[ºC] and 600[ºC]. From this time, temperatures rise suddenly, in wood, due to the large quantity of flame production. The velocity propagation depends on characteristics of the material, the shape of the parts and the surrounding conditions, [22-26]. The full development phase, which occurs during combustion of all combustible materials and the temperature, remains constant, [26-27]. Finally, the extinction phase or cooling phase,

due to a decrease in the temperature, or the fuel shortage or lack of oxygen, which may lead to extinguishing the fire, [26-27].

2.3.1 Standard time-temperature curve

The evolution of the fire temperature is defined according to the rated temperature curves as a function of time, or another shape as parametric curves defined for this purpose, according Eurocode 1 part 1.2, [16]. The fire curve ISO834 allows the development of the room temperature [28]. This curve is described by the equation 11 and represented in figure 6:

$$T = T_0 + 345\log_{10}(8t + 1) \tag{11}$$

Where **T** is the gas temperature in the compartment [°C], **t** is the time in [min] and $\mathbf{T_0}$ is the initial temperature compartment, which usually is considered equal to 20[°C].

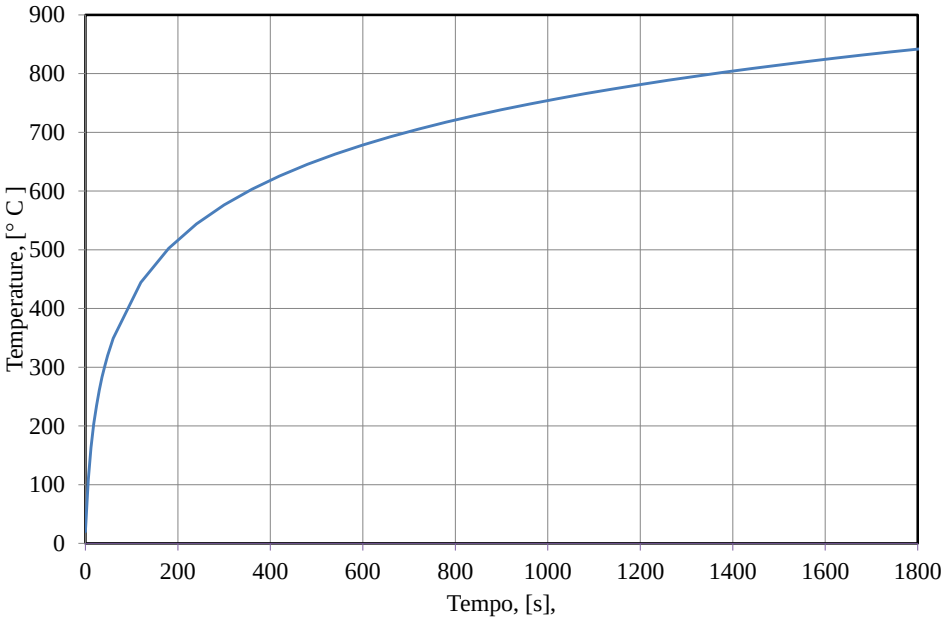

Figure 6- Standard time-temperature curve ISO 834, [6].

2.3.2 External fire curve

The external fire curve shown in Eurocode 1 part 1.2 [16], applies only for external structural elements, and the temperature is described by the equation:

$$T = 660 \times \left[1 - 0.687e^{-0.32t} - 0.313e^{-3.8t}\right] + T_0 \quad (12)$$

In this equation after 30 [min], temperature keeps constant at 680 [ºC]. The others parameters are **T** representing the gas temperature near the member in [°C] and **t** is the time in [min].

2.3.3 Hydrocarbon curve

The hydrocarbon curve is defined by equation 13, that is a curve which is characterized as the most energetic of all, after 30[min] the temperature remains constant to 1100[° C] according to Eurocode 1 part 1.1, [16] the equation is given by:

$$T = 1080 \times \left[1 - 0.325e^{-0.167t} - 0.675e^{-2.5t}\right] + T_0 \quad (13)$$

Where: **T** is the gas temperature in the fire compartment in [°C], **t** is the time [min].

2.3.4 ASTM fire curve

Based on ASTM E119, [17], equation 14 characterizes the temperature evolution according to ASTM fire curves, which is used to test the behaviour of structural elements to fire.

$$T = 750 \times \left[1 - e^{-3.79553\sqrt{t}}\right] + 170.41 \times \sqrt{t} + T_0 \qquad (14)$$

Where **t** represents the time elapsed since the start of the test in [min] and $\mathbf{T_0}$ the initial temperature of the enclosure in the [°C].

In figure 7, different curves are represented, according to the evolution of temperature versus time history.

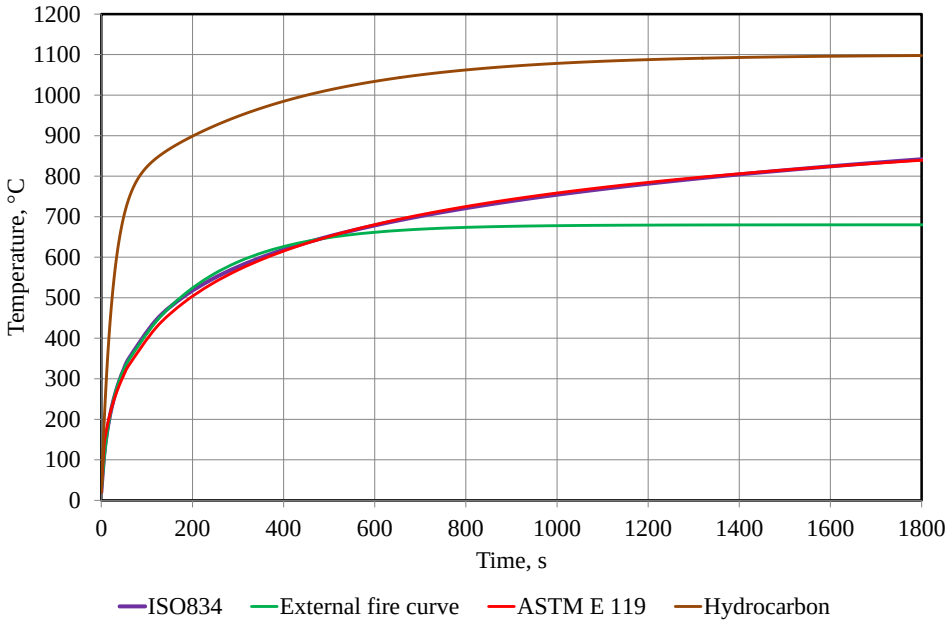

Figure 7- Standard fire curves.

For the fire resistance of structural elements, usually the standard fire curve ISO 834, [6] is used. Although with little physics reality, it allows standardizing experimental tests, enabling the comparison of the results of fire resistance obtained in different laboratories, [29].

Chapter 3

Thermal Behaviour

3 Thermal Behaviour

Fire is one of the great opponents of the building materials, which can be the first responsible for losing stiffness and strength for some materials like steel, also for wood when it's exposure to high temperatures the section gradually reduces, [27]. The timber is characterized by his low thermal conductivity. This property is used to delay the increase in temperature in the vicinity of areas that is in the combustion and prevent excessive expansion of the structure. When wood is exposed to fire, three different layers can be distinguished over the section, figure 8. The first layer is the surface characterized by carbonization. This layer function plays a role as a good thermal insulation due to its low thermal conductivity, preventing the penetration of heat into the section. The pyrolysis zone is a layer located between the charred layer and the wood core, usually with smaller thickness, where the properties are changed, but not completely decomposed. The last zone is defined inside the section where the wood does not suffer any change in its properties. This zone is the intact wooden zone, [27], [30].

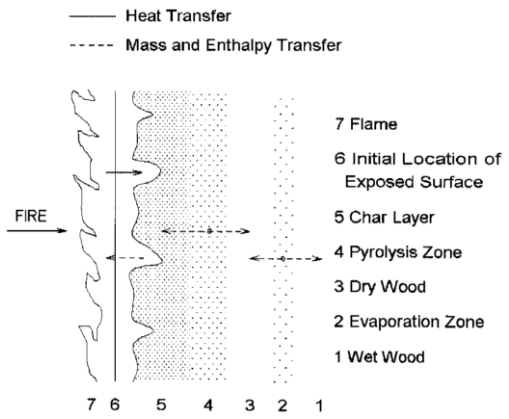

Figure 8- Physical degradation zones in a wooden section, [31].

3.1 Pyrolysis

Pyrolysis is a process of wood degradation when subjected to high temperatures and an environment devoid of oxygen. When wood is heated in a controlled atmosphere to 100[°C], very few chemical reactions happens. From this temperature the evaporation of the existing

moisture occurs. As the temperature is raised to 200[°C] the surface layer of the wood starts to dehydrate in the absence of oxygen, this process of thermal degradation level is called pyrolysis, between 200[°C] and 280[°C], and the degradation of the surface layer moves to the inside of the timber. This region is followed by a layer in which the pyrolysis takes place slowly. Between 240[°C] and 350[ºC] there is a slow formation of char layer. In the range between 280[°C] to 500[°C], exothermic reactions produce with the release of combustible gases, in the form of smoke. Above 500[°C] it remains in the temperature elevation, to complete char layer, [28].

3.1.1 Ignition

The wood ignition happens when it is subjected to an enough high temperature with oxygen-rich atmospheres. Ignition may be two distinct types: spontaneous or provoked. Spontaneous happen in the absence of any ignition source, and the surface of the wood is ignited by any means of energy, a heat of a fire or a burning object. This flux of energy or heat may have two components, radiation and convection. The provoked ignition happens when the wood surface reaches into contact with any source of ignition, flame or spark, [28].

3.1.2 Char layer of wood

When subjected to high temperatures, wood suffers a breakdown and the formation of a layer of carbon happens. This layer plays the role of insulation which slows their degradation. Also there are several analytic models to calculate the thickness of the wood char layer. The Eurocode 5 part 1.2, [15] proposes design equations for determining the evolution of the thickness dchar,$_0$ [mm] carbonization figure 9, in a non-protected structure during fire exposure, as shown in equation 15, [15].

$$d_{char,0} = \beta_0 \times t \tag{15}$$

Where **t** is the time of fire exposure [min] and β_0 is the charring rate on [mm/min].

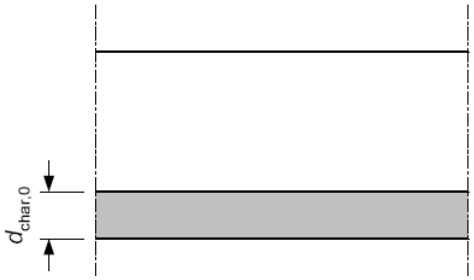

Figure 9- One-dimensional char layer of a cross section (fire exposure on one side), [15].

The depth of carbonization calculated by equation 15 does not consider the rounding of corners and the cracks in the wood, figure 10. It is necessary to use another equation to calculate the evolution of the char layer, equation 16 as described in Eurocode 5 part 1.2, [15].

$$d_{char,n} = \beta_n \times t \tag{16}$$

Where $\mathbf{d_{char,n}}$ is the design char layer depth, which incorporates the effect of corner rounding, $\boldsymbol{\beta_n}$ is the notional design charring rate, the magnitude of which includes for the effect of corner rounding and cracks.

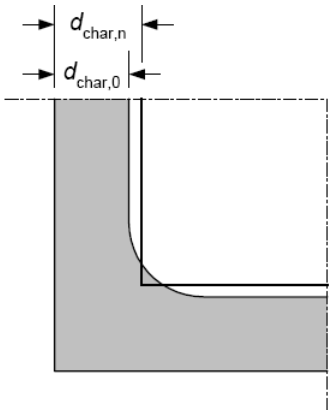

Figure 10- Char layer depth when fire exposure more than one side, [15].

Eurocode 5 part 1.2, [15], proposes values to consider the charring rate, depending on the density and type of wood, as shown in Table 1.

Table 1: Design charring rates β0 and βn of timber, [15].

Type of wood	β_0	β_n
a) Softwood and beech		
Glued laminated timber with a density of ≥ 290 kg/m^3	0.65	0.70
Solid timber with a density of ≥290 kg/m^3	0.65	0.80
b) Hardwood		
Solid or glued laminated hardwood with a density of 290 kg/m^3	0.65	0.70
Solid or glued laminated hardwood with a density of ≥ 450 kg/m^3	0.50	0.55

3.1.3 Effective char layer

Calculating the effective char layer according Eurocode 5 part 1.2 [15], records the thickness resulting from the pyrolysis, as defined in equation 17 and represented in figure 11:

$$d_{eff} = d_{char,n} + k_0 \times d_0 \tag{17}$$

with, $\boldsymbol{d_0}$ is equal to 7 mm and $\boldsymbol{d_{char,n}}$ is the char layer depth determined according to equation 16.

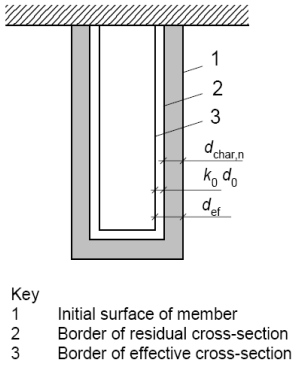

Figure 11- Definition of residual cross-section and effective cross-section, [15].

For unprotected surfaces, k_0 should be determined from table 2, [15].

Table 2: Determination of k_0 for unprotected surfaces with t in minutes, [15].

Time	k_0
$t \leq 20$ min	t/20
$t \geq 20$ min	1

For unprotected surfaces figure 12a, for protected surfaces with $\mathbf{t_{ch}} > 20$ minutes, it should be assumed that $\boldsymbol{k_0}$ varies linearly from 0 to 1 during the time interval from $\mathbf{t} = 0$, to $\mathbf{t} = t_{ch}$, figure 12b. For protected surfaces with $\boldsymbol{t} \leq 20$ minutes, it is necessary applies the table 2.

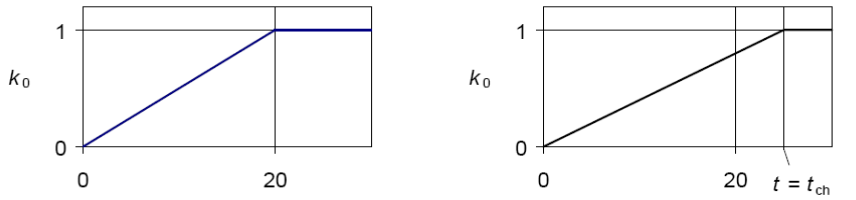

a) b)

Figure 12- Variation of k_0: a) for unprotected members and protected members where $t_{ch} > 20$ minutes, b) for protected members where $t_{ch} > 20$ minutes.

3.2 Thermal properties of wood

The thermal properties of wood vary according to the material temperature. The variations of thermal properties play a considerable role in the calculation of char depth as a function of time, [18].

The thermal properties of wood (specific heat, density and thermal conductivity), which are defined in Annex B [15] are conditioned by the ambient temperature, which should consider temperature equal to 20°C at the initial wood moisture content of 12 % and standard fire conditions, regardless of species of wood.

3.2.1 Thermal conductivity

Thermal conductivity is a time rate of energy transmission in the form of heat flow through material subjected to a temperature gradient. The thermal conductivity of wood structural elements is small compared to the others materials like steel, [26].

Table 3 and figure 13 represent the temperature dependent thermal conductivity, [15].

Table 3: Temperature-thermal conductivity relationship for wood, [15].

Temperature [°C]	Thermal Conductivity [W/mk]
20	0.12
200	0.15
350	0.07
500	0.09
800	0.35
1200	1.5

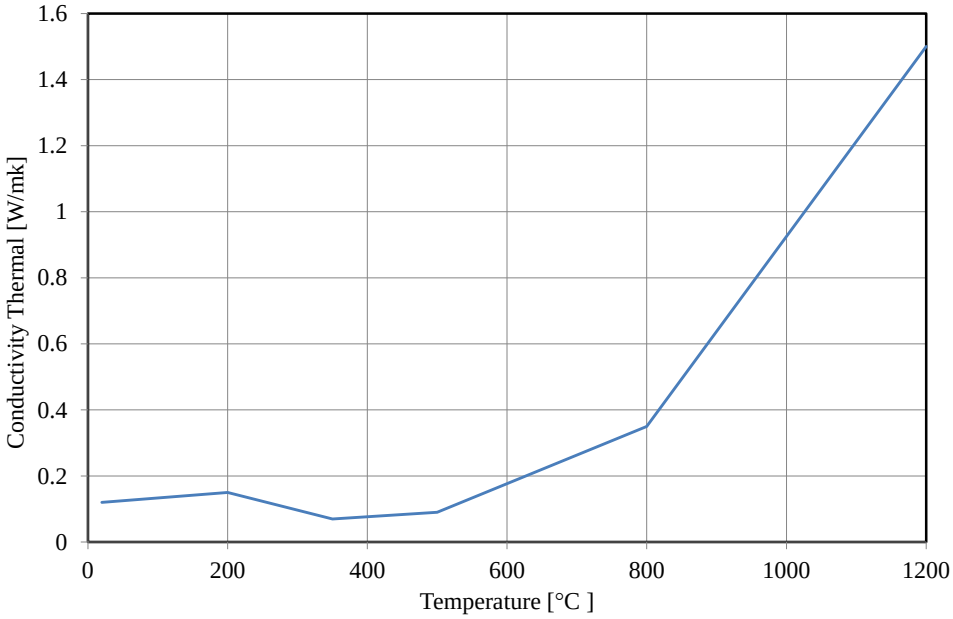

Figure 13- Thermal conductivity as a function of temperature.

3.2.2 Specific heat

The specific heat is a physical quantity that defines the thermal variation of a substance when receiving heat. The specific heat depends to the moisture content and the temperature, but does not vary between species or even with the density.

The property values are shown in Table 4 and figure 14, as values of Eurocode 5, [15].

Table 4: Specific heat of wood, Eurocode 5, [15].

Temperature [°C]	Specific heat [kJ/kgK]
20	1.53
99	1.77
99	13.60
120	13.50
120	2.12
200	2.00
250	1.62
300	0.71
350	0.85
400	1.00
600	1.40
800	1.65
1200	1.65

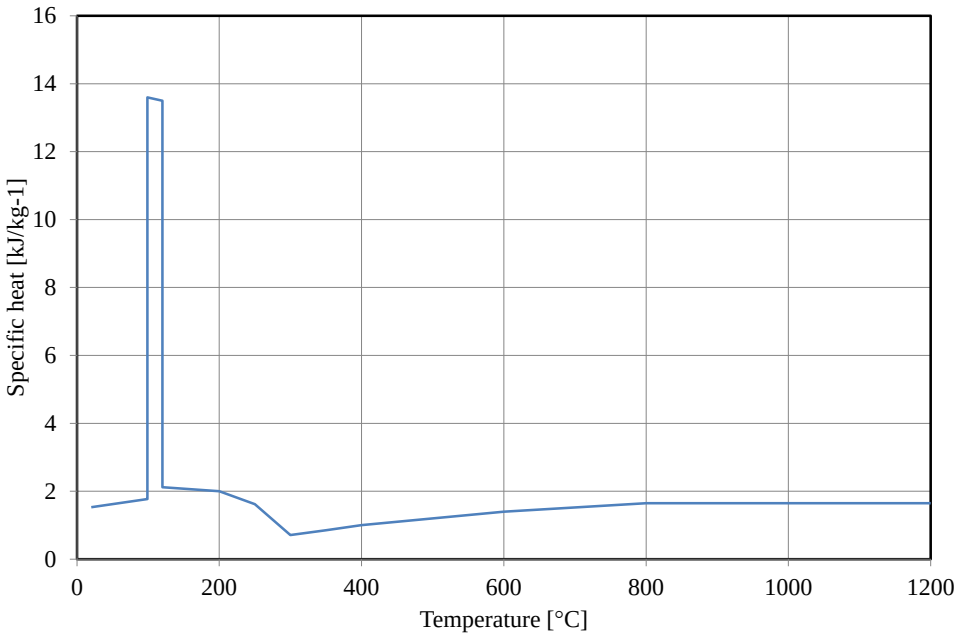

Figure 14- Specific heat as a function of temperature.

3.2.3 Wood density

The timber has a density which is related to the moisture content which affects their behaviour according to Eurocode 5, [15]. Table 5 shows the values considering an average humidity **(w)** of 12%. Figure 15 shows the density coefficient as a function of temperature according Eurocode 5 part 1.2. In this study, the value of density is equal to 450[kg/m^3] at room temperature, represent of a spruce material.

Table 5: Specific mass of wood, Eurocode 5, [15].

Temperature [C°]	Density Coefficient
0	1+w
99	1+w
99	1+w
120	1.00
120	1.00
200	1.00
250	0.93
300	0.76
350	0.52
400	0.38
600	0.28
800	0.26
1200	0.00

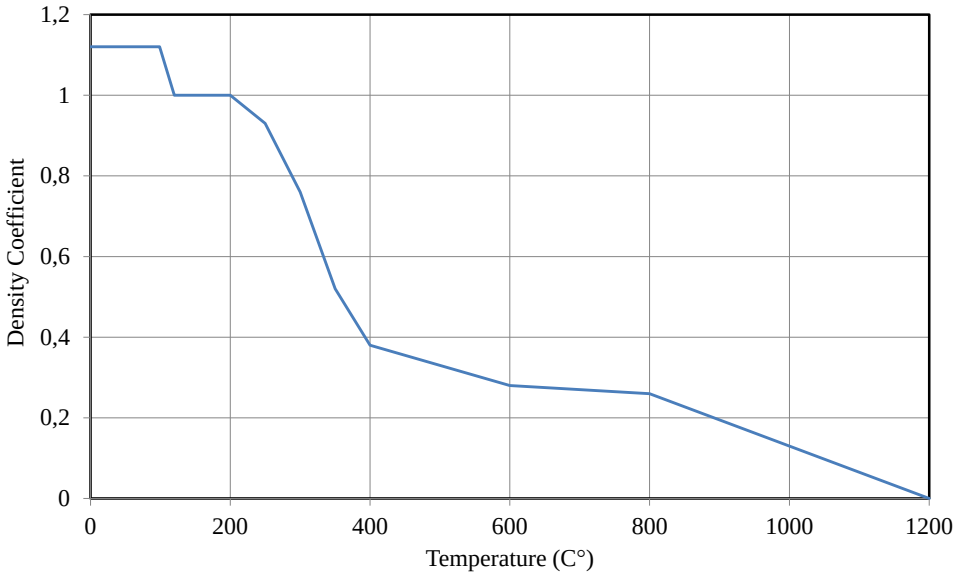

Figure 15- Density coefficient as a function of temperature.

3.3 Thermal properties of insulation materials

Insulation materials are building materials which reduce the heat transfer to other elements. They may be categorized by its composition (natural or synthetic materials), form (spray foam, panels …), structural effect, functional mode, resistance to heat transfer, environmental impacts, etc. The choice of which insulation material is used depends on a wide variety of factors. The factors affecting the type and amount of insulation to be used in a building include: thermal conductivity; moisture, strength, ease of installation, durability, cost, toxicity, flammability, also environmental impact and sustainability.

There are different insulation materials: Rockwool, ceramic fibre, calcium silicate boards, gypsum boards, intumescent materials, spray-on cement based materials. Depending on the application or in conjunction with others materials, the selection of the insulation material will be the guarantee to produce better thermal performance. The important thermal properties of the insulation materials are: thermal conductivity, density and specific heat.

The medium density fibreboard (MDF) is a wood-based panel composed of wood fibres that are mixed with resin and pressed into flat panels under high temperature and pressure. Typical applications of MDF are furniture, shelving, laminate flooring, decorative mouldings, office dividers, walls and ceilings, house construction, sliding doors, kitchen worktops, interior signage, and other industrial products. The material production is increasing due to the development of manufacturing technologies, figure 16. MDF products are used for traditional wood applications that require fungal resistance. This study investigated some of the important biodegradation properties of MDF composite board made from renewable biomass from pineapple leaf fibre, [32]. Nerveless MDF material is combustible, and the level of fire resistance depends of their density.

Mineral wool, as mineral fibre, mineral cotton, mineral fibre, man-made mineral fibre, and man-made vitreous fibre, is a general name for fibre materials that are formed by spinning or synthetic minerals. Specific mineral wool products are stone wool and slag wool. Europe also includes glass wool which, together with ceramic fibre, is completely man-made fibres. Applications of mineral wool include thermal insulation, filtration, soundproofing, and hydroponic growth medium. At times, it is used incorrectly the rockwool name as synonym for mineral wool. But, Rockwool is a registered trademark by the Danish company Rockwool International. Mineral wool (RW) insulations are boards designed for high temperature applications where durability and compressive resistance are required, in a variety of densities. The applications including storage tank insulations, drying/oven equipment and petro-chemical and power generating equipment protection. This insulation material is designed for high temperature applications, good compressive resistance, excellent fire resistance properties, non-combustible, melting point of approximately 1177[°C] [33], and chemically inert.

Other typical insulation material is the gypsum board. This material is a typical panel that consist of a non-combustible core, composed primarily of gypsum, and a paper surfacing on the face, back and long edges, used in as several building materials. Gypsum board walls

and ceilings have different advantages: ease of installation, fire resistance, sound isolation, and durability.

According to technical information, fiberglass is the most common insulation material used. Because of its processing stage, fiberglass is able to minimize heat transfer. The main downside of fiberglass is the danger of handling it, and can cause damage to the eyes, lungs, and even skin. Nevertheless, when the proper safety equipment is used, fiberglass installation can be performed. Fiberglass is a non-flammable insulation material. Mineral wool actually refers to several different types of insulation. Most mineral wool does not have additives to make it fire resistant, and it is not combustible. When used in conjunction with other, mineral wool can definitely be an effective way of insulating large areas.

Figure 16- Medium fibre density and mineral wool [34].

In our study, MDF and RW will be applied in the wooden slab to verify the increased resistance to insulation considering the material properties in table 6.

Table 6: Overview of the insulation material properties.

Insulation Materials	Conductivity [W/mk]	Specific Heat [J/kgK]	Density [kg/m^3]	Emissivity	Temperature range	Thermal diffusivity $\alpha = \lambda / (\rho\, cp)$, x10^{-7} [m^2/s]
Mineral wool, RW [35] (Non-combustible)	0.04	840	100	0.90	760-1400	4.76
Fibreglass [36]	0.04	1000	25	0.75	-30 to 540	16.00
Fibre board [36] (Non-combustible)	0.06	1000	300	0.85		2.00
Gypsum board [37] (No combustible)	0.17	1090	1442	0.85		1.08
Medium fibre density, MDF [11] (Combustible)	0.14	1700	600	1.00	300	1.37

3.4 Thermal properties of air

The air is a mixture of different gases, mainly nitrogen and oxygen, but it contains much smaller amounts of water vapour, argon, carbon dioxide, and very small amounts of other gases. Air also contains spores, suspended dust and bacteria. Because of the wind action, the composition of air varies only a little with altitude and location, [38]. The thermal properties of air are given from the table 7. The air properties will be considered in our study, in the wooden slab with cavities and insulation material.

Table 7: Thermal properties of air, [39].

Temperature	Density [kg/m^3]	Specific heat [J/kgK]	Thermal conductivity [W/mk]
20	1.166	1000	0.0258
30	1.127	1000	0.0265
40	1.091	1000	0.0272
50	1.057	1000	0.0279
60	1.026	1001	0.0299
70	0.996	1001	0.0292
80	0.967	1001	0.0299
90	0.941	1001	0.0306
100	0.916	1001	0.0312
120	0.869	1001	0.0324
140	0.827	1002	0.0349
160	0.789	1002	0.0349
180	0.754	1002	0.0362
200	0.722	1003	0.0374
250	0.6530	1003	0.0406
300	0.5960	1005	0.0437
350	0.5482	1006	0.0464
1000	0.5482	1006	0.0464

Chapter 4

Finite Element Method

4 Finite Element Method

4.1 Introduction

The finite element method is a numerical technique used to solve various problems which are attached by partial differential equations or can be formulated as functional minimization. A domain of interest is represented as an assembly of finite elements. Approximating functions in the finite elements are given in terms of nodal values of a physical field which is required. A continuous physical problem is transformed into a discretized finite element problem with unknown nodal values. For a linear problem a system of linear algebraic equations should be solved. Values inside finite elements can be recovered using nodal values, [40].

In this work, Ansys program will be used, as a finite element method, normally used to solve structural analysis, fluid dynamics, explicit and implicit methods and heat transfer. According to the numerical simulations, the thermal analysis will be used including the non-linear behaviour of the materials and the transient heat effect.

4.2 Equations and boundary conditions

For an isotropic body with temperature dependent, it is necessary to understand the heat transfer processes. In order to know the distribution of temperature in structural elements, the heat transfer is given by a basic equation as the following appearance:

$$\frac{\partial}{\partial x}\left(\lambda\frac{\partial T}{\partial x}\right)+\frac{\partial}{\partial y}\left(\lambda\frac{\partial T}{\partial y}\right)+\frac{\partial}{\partial z}\left(\lambda\frac{\partial T}{\partial z}\right)+Q=\rho C_p\frac{\partial T}{\partial t} \tag{18}$$

Where **λ** is the thermal conductivity, $\mathbf{C_p}$ is the specific heat of the material, **ρ** is the specific mass of the material, and **T** is the temperature field and **t** the time.

This expression shows that the net amount of energy, transferred by conduction inside of the unit volume, for any point of the volumetric flow rate, is equal to the rate of change

thermal energy stored within this volume. For this, it is necessary to solve the problem using the initial and their boundaries conditions [26], shown in Figure 17.

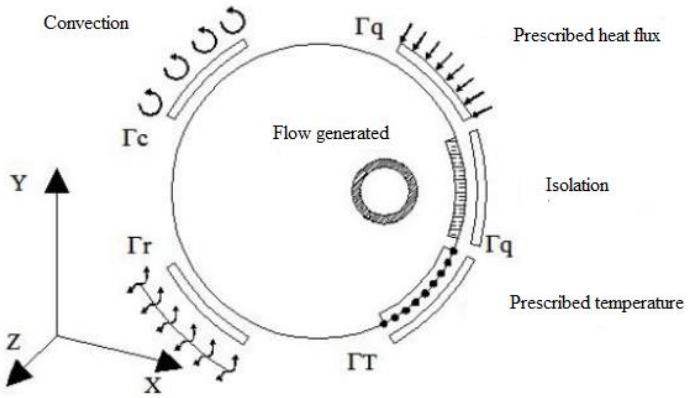

Figure 17- Boundary conditions for thermal problems in the field Ω, [41].

With the equation 18 it is possible to point out the thermal diffusivity α which determines the temperature distribution in non-steady or transient conditions, given by equation 19. In heat transfer analysis, the thermal diffusivity is the conductivity divided by the density and the specific heat.

$$\alpha = \lambda / (\rho \, C_p) \tag{19}$$

Thermal diffusivity measures the ability of a material to transmit a thermal disturbance or to conduct thermal energy relative to its ability to store thermal energy. It indicates how quickly the temperature in the material changes. Substances with high thermal diffusivity rapidly adjust their temperature to that of their surroundings, because they conduct heat quickly in comparison to their volumetric heat capacity.

Using the finite element method to discretize the problem in domain, a weak formulation based in Galerkin method is used, for choosing the weighting functions. This allows the following system of differential equations represented in equation 20 or 21, [42].

$$\mathbf{K}_{(\lambda)(T,t)}\, T_{(t)} + \mathbf{C}_{(Cp,\,\rho)}\, T^{*}_{(t)} = \mathbf{F}_{(T,t)\,(Q,q,hcr,Tp)} \tag{20}$$

$$\mathbf{K}\mathbf{T} + \mathbf{C}\dot{\mathbf{T}} = \mathbf{F} \tag{21}$$

Each term of the equation 21 could be represented in terms of the following expressions:

$$K_{lm} = \sum_{e=1}^{E} \int_{\Omega^e} \left(\nabla N_l \lambda \nabla N_m\right) d\Omega^e + \sum_{e=1}^{H} \int_{\Gamma_h^e} h_{cr} N_l N_m d\Gamma_h^e \tag{22}$$

$$C_{lm} = \sum_{e=1}^{E} \int_{\Omega^e} \rho c_p N_l N_m \, d\Omega^e \tag{23}$$

$$F_l = \sum_{e=1}^{E} \int_{\Omega^e} N_l \dot{Q} d\Omega^e - \sum_{e=1}^{Q} \int_{\Gamma_q^e} N_l \bar{q} \, d\Gamma_q^e + \sum_{e=1}^{H} \int_{\Gamma_h^e} N_l h_{cr} \theta_\infty \, d\Gamma_h^e \tag{24}$$

Where E is the total number of elements, Q is the number of elements with boundary type Γ_q, H is the number of elements with boundary type Γ_c and/or Γ_r, N_l and N_m are typical shape functions.

In the present work for two dimensional analyses an element with eight nodes and with parabolic shape functions will be used. For three dimensional analyses, linear shape functions will be used, due the solid element choosed, with eight nodes.

Using a finite difference technique to discretize the time, the system of ordinary differential equations (21) results in the recurrence formula, [42]:

$$\hat{\mathbf{K}}_{n+\alpha} \mathbf{T}_{n+\alpha} = \hat{\mathbf{F}}_{n+\alpha} \qquad 0 < \alpha \leq 1 \tag{25}$$

where

$$\hat{\mathbf{K}}_{n+\alpha} = \mathbf{K}_{n+\alpha} + \frac{1}{\alpha \Delta t} \mathbf{C}_{n+\alpha} \tag{26}$$

$$\hat{\mathbf{F}}_{n+\alpha} = \mathbf{F}_{n+\alpha} + \frac{1}{\alpha \Delta t} \mathbf{C}_{n+\alpha\, n} \tag{27}$$

Having solved the system of equations (25) for $\mathbf{T}_{n+\alpha}$, at time $t_{n+\alpha}$, the value of $\mathbf{T}$ at the end of the time interval Δt, that is, at time t_{n+1} is given by

$$\mathbf{T}_{n+1} = \frac{1}{\alpha}\mathbf{T}_{n+\alpha} + \left(1 - \frac{1}{\alpha}\right)\mathbf{T}_n \tag{28}$$

The value of the parameter α could varies using the Crank-Nicolson scheme with $\alpha = 1/2$, using the Galerkin scheme with $\alpha = 2/3$ and using the Euler Backward scheme for $\alpha = 1$.

In non-linear problems, where the thermal properties of the material are temperature dependent, the system of equations (21) can generally be written as:

$$\mathbf{K}(\mathbf{T},t)\mathbf{T}(t) + \mathbf{C}(\mathbf{T},t)\dot{\mathbf{T}}(t) = \mathbf{F}(\mathbf{T},t) \tag{29}$$

There is not a general method to solve this system of non-linear differential equations. However, several numerical solution procedures, in essence, based on linear time integration and an iterative process are available, [42], [16]. In general, an effective algorithm for the analysis of non-linear transient thermal problem is used. The matrices **K** and **C** and the vector **F**, can vary throughout the time interval Δt as functions of the unknown vector temperature **T** or **T** and time *t*. Therefore, these matrices must be evaluated at time $t_{n+\alpha}$ and the temperature $\mathbf{T}_{n+\alpha}$.

In order to fully satisfy these non-linear conditions of the problem, it is necessary to employ an iterative procedure in each time step. In this algorithm a modified Newton-Raphson method is used. During any step, *i*, of the iterative process of solution, the equation will not generally be satisfied unless convergence has occurred. Therefore a system of residual forces $\boldsymbol{\psi}$ will exist:

$$\boldsymbol{\psi}^{i}_{n+\alpha} = \hat{\mathbf{F}}^{i}_{n+\alpha} - \hat{\mathbf{K}}^{i}_{n+\alpha}\mathbf{T}^{i+1}_{n+\alpha} \neq 0 \tag{30}$$

The improved value of $\mathbf{T}^{i+1}_{n+\alpha}$ can be obtained. And the iterative procedure is then continued, solving a set of linearized equations at every iteration step, until the solution converges to the non-linear solution. The convergence criteria employed is as follows:

$$\frac{\left\|\Delta \mathbf{T}_{n+\alpha}^{i}\right\|}{\left\|\mathbf{T}_{n+\alpha}^{i+1}\right\|} < TOL \tag{31}$$

Where: *TOL* is the specified tolerance equal to 0.001 used in ANSYS© program, $\|\cdot\|$ denotes the Euclidean vector norm, $\Delta \mathbf{T}_{n+\alpha}^{i}$ is the temperature change in the i^{th} iteration and $\mathbf{T}_{n+\alpha}^{i+1}$ is the current temperature value.

4.3 Finite elements

The finite element method is very used for the approximation of the numerical solutions for differential equations. By this "reason", a finite element formulation must be carried out using a system of algebraic equations, as is the case of the finite element program used in this work.

The finite element Plane77 with 8 nodes is used for 2D, with one degree of freedom, temperature, at each node, figure 18. The element is applicable for thermal and nonlinear material in transient analysis, [43].

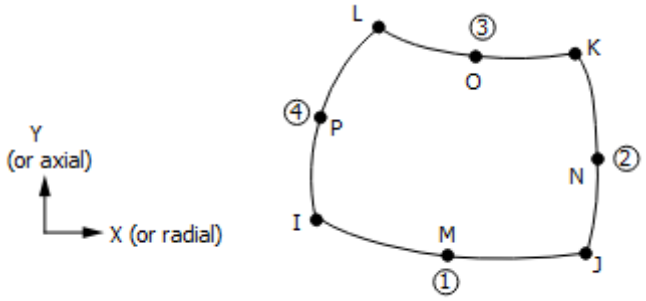

Figure 18- PLANE77 geometry, [43].

A 3D finite element (Solid90) with 20 nodes, with single degree of freedom for temperature, was used for nonlinear transient thermal analysis, [43], as represented in figure 19.

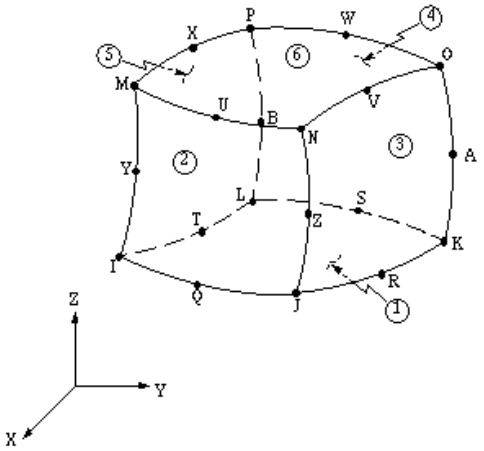

Figure 19- SOLID90 3-D 20-Node Thermal Solid [43].

4.3.1 Shape functions for 8 nodes (Lagrange)

Quadratic two-dimensional isoparametric finite elements are presented in Figure 18. Shape functions Ni are defined in local coordinates ξ, η (−1 ≤ ξ, η ≤ 1), [40]. The term ”isoparametric” means that geometry and temperature field are specified in parametric form and are interpolated with the same functions. Both coordinates and temperature are interpolated with the same shape functions, [40].

Shape functions for 8 nodes are presented in the following:

For i= I, J,K, L:

$$N_i = \frac{1}{4}(1+\xi_0)(1+\eta_0) - \frac{1}{4}(1-\xi^2)(1+\eta_0) - \frac{1}{4}(1+\xi_0)(1-\eta^2) \tag{32}$$

For i= M, O:

$$N_i = \frac{1}{2}(1-\xi^2)(1+\eta_0) \tag{33}$$

For i= P, N:

$$N_i = \frac{1}{2}(1+\xi_0)(1-\eta^2) \tag{34}$$

In the above equations the following notation is used: ξ0 = ξξi, η0 = ηηi where ξi, ηi are values of local coordinates ξ, η at nodes.

4.3.2 Shape functions for 20 nodes (Serendipity)

Hexahedral (or brick-type) linear 8-node and quadratic 20-node three-dimensional isoparametric elements are depicted in figure 19. Shape functions used for interpolation are polynomials of the local coordinates ξ, η and ζ ($-1 \leq \xi, \eta, \zeta \leq 1$).

The shape functions of the 20-node hexahedron can be grouped as follows. For the corner nodes i = I, J, K, L, M, N, O, P:

$$N_I^{(e)} = \frac{1}{8}(1+\xi\xi_i)(1+\eta\eta_i)(1+\mu\mu_i)(\xi\xi_i+\eta\eta_i+\mu\mu_i-2) \tag{35}$$

For the midside nodes *i* = Q, S, U, W:

$$N_I^{(e)} = \frac{1}{4}(1-\xi^2)(1+\eta\eta_i)(1+\mu\mu_i) \tag{36}$$

For the midside nodes i = R, T ,V, X:

$$N_I^{(e)} = \frac{1}{4}(1-\eta^2)(1+\xi\xi_i)(1+\mu\mu_i) \tag{37}$$

For the midside nodes i = Y, Z, A ,B:

$$N_I^{(e)} = \frac{1}{4}(1-\mu^2)(1+\xi\xi_i)(1+\eta\eta_i) \tag{38}$$

It is very easy to observe that the shape functions have the delta function property. The shape function is constructed by simple inspections, making use of the shape function properties.

Chapter 5

Cellular Slab With Perforations

5 Cellular Slab With Perforations

5.1 Introduction

The wooden slabs are structural elements with increasing use in the rehabilitation of structures. For some spaces sound insulation is a key requirement like, restaurants, schools, and wood material present this characteristic. Perforations and cellular wooden slabs drew attention of experts, due their architecture, light weight, services installation and also an easy maintenance.

The construction system of the cellular slab is based on a combination of a wood panel for floor and ceiling structures, disassociated by beams, as represented in figure 20. Combining quality materials with good technique construction allow to obtains solutions as a pleasant an aesthetic lightness and safety for use. Also boards cells with slight perforations are easy to come up with great architectural features, thermal and acoustic conditions, [27].

Figure 20- Constructive models of wooden slabs, [27].

5.2 Dimensions of the perforated wooden slab

In this work, wooden cellular slabs were considered for analysis. These construction models were based on the dimensions of constructive solutions and tested in previous experimental work in the Polytechnic Institute of Bragança, [14]. The bottom surface of the slab (perforated side) was submitted to a fire action, [14]. The construction model considers a wooden perforated slab with dimensions equal to (870×996.8×32) [mm]. The top wooden surface is solid (1150x1232) [mm] with homogenous thickness 19[mm]. The geometric model

of each slab considers three different cellular zones (two cells with different perforations and one cell with no perforation), [11], represented in figure 21.

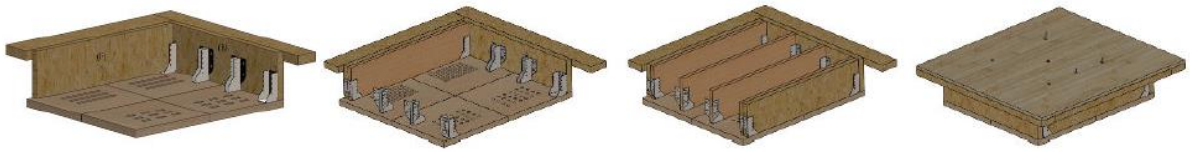

Figure 21- Wooden slab with cellular zones, [14].

The slabs present in the exposed surface two types of rectangular perforations (250x20) [mm] in cell 3, and (50× 20) [mm] in cell 1. Other slabs present circular perforations with a diameter equal to 20[mm] in cell 3, and 10[mm] in cell 1

5.3 2D cellular slab with perforations

5.3.1 Presentation of models and geometry

In this work only the two-dimensional (2D) slab cross-sections with perforations were considered for analysis, as the previous slab dimensions. The cross-section includes three different cellular zones (two with perforations and one without perforations).

Figure 22 represents all technical drawing of the models with all considered dimensions. Autocad was the program chosen to represent and produces all these drawings.

The wooden cellular slab in study has different types of perforations (R rectangular or D circular) at the bottom. Also, additional 2D models will be considered with internal insulation material (MDF and RW). The MDF and RW were added inside the perforated cavities and considered with different sizes (18mm or 36mm), as shown in figure 22. Due to the combination between materials and slab geometries, numerical models were solved. For each model, one side was considered exposed to fire scenario and the time-temperature history was obtained during one half hour of fire exposure.

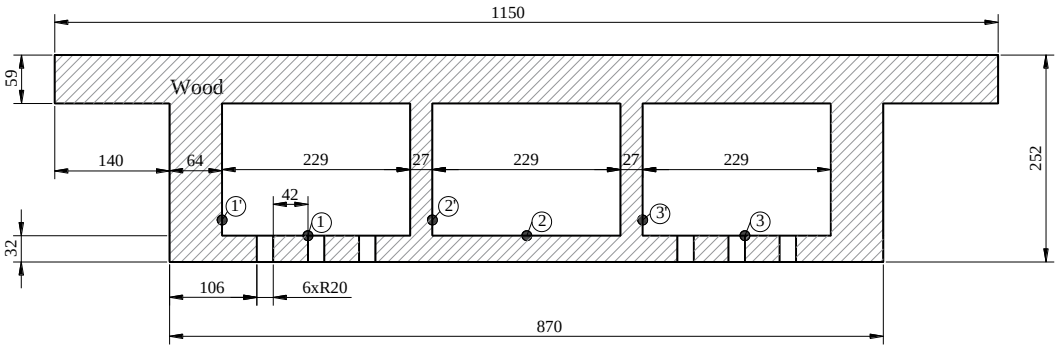

Figure 22- a) Wooden cellular slab: rectangular perforation.

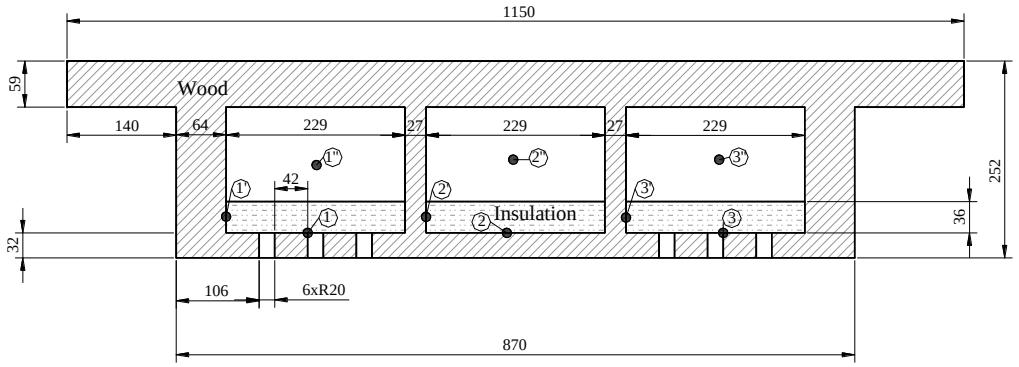

Figure22- b) Wooden cellular slab: rectangular perforation with 36 mm of (MDF), (RW).

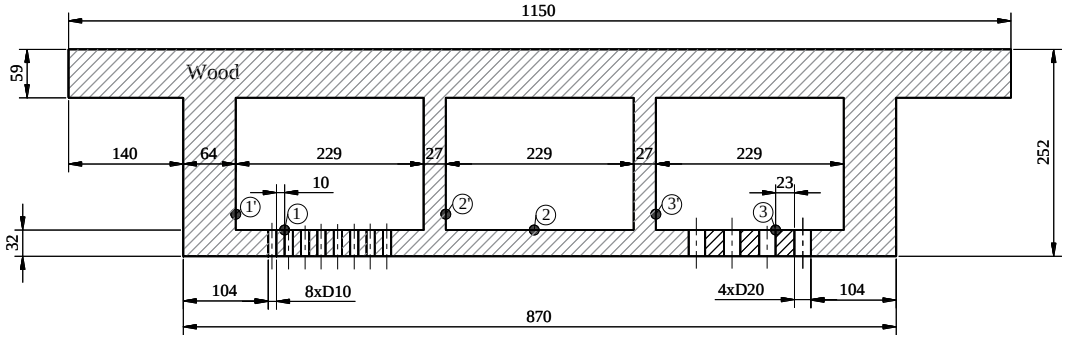

Figure22- c) Wooden cellular slab: circular perforation.

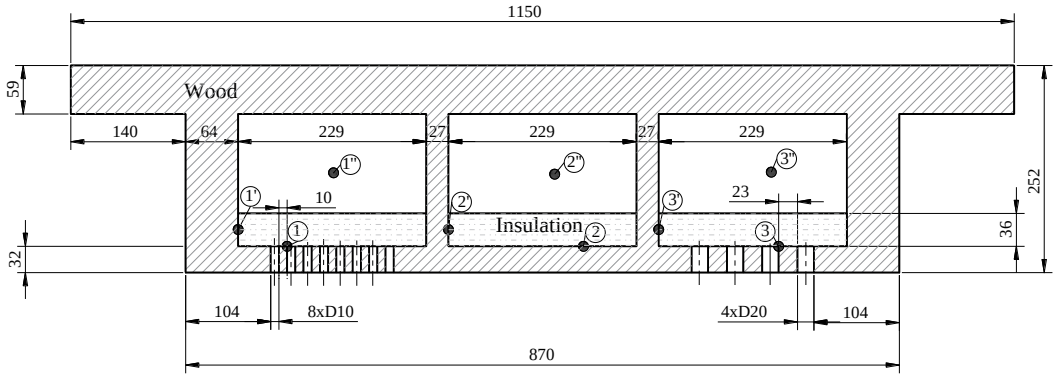

Figure22- d) Wooden cellular slab: circular perforation with 36mm of (MDF), (RW).

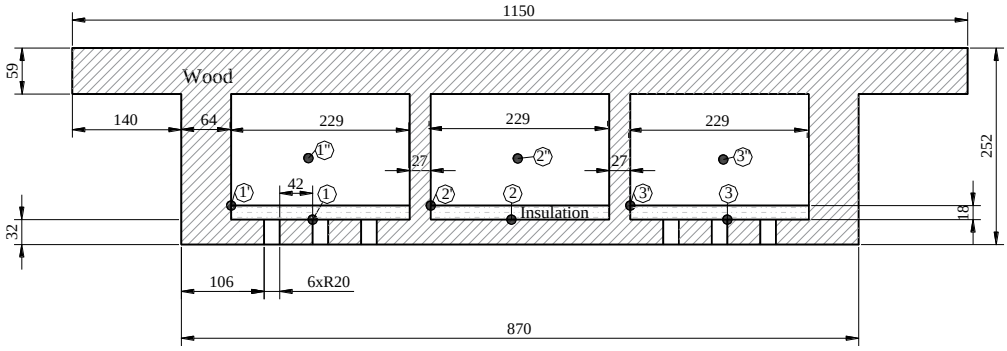

Figure22- e) Wooden cellular slab: rectangular perforation with 18mm of (MDF), (RW).

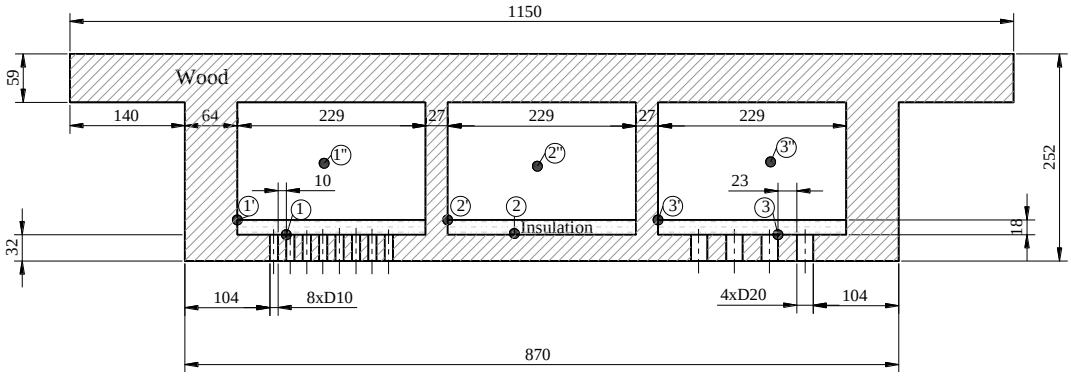

Figure22- f) Wooden cellular slab: circular perforation with 18mm of (MDF),(RW).

The nonlinear transient numerical analysis was carried out to 1800[s] according to the experimental fire exposure

For this work different numerical models were defined as represented in table 8.

Models 1 to 6 consider the applied ISO 834 standard fire at the perforated bottom surface .These models will be implemented and compared with the models 7 to 12, where the exposure fire ‘’Furnace’’ as the same behaviour like in the experimental tests in laboratory [14]. The main goal was to simulate in 2D analysis the same occurrence as in 3D experimental. Models 7 and 9 permit to conclude about the use of the 2D model as an alternative when compared with the same behaviour in 3D experimental tests.

Also, other numerical comparison will be produced between models with the typical boundary condition ‘’Furnace’’ and the ISO 834 fire, due the new introduction of the insulation material effect in wood material, with different applied external conditions. According to this, all the remaining and more additional 2D models could be used with more performance and with different proposal (different insulation materials and board sizes) to obtain different conclusions for building wooden slab applications.

Table 8: Numerical models characterizations.

Models	**Number of Figures**	**Geometrics**	**Boundary Conditions**
Model 1	Figure 22.a)	Rectangular	ISO 834
Model 2	Figure 22.b)	Rectangular with MDF=36mm Rectangular with MDF=36 mm, internal air Rectangular with RW=36mm Rectangular with RW=36mm, internal air	
Model 3	Figure 22.c)	Circular	
Model 4	Figure 22.d)	Circular with MDF=36mm Circular with MDF=36mm, internal air Circular with RW=36mm, internal air	
Model 5	Figure 22.e)	Rectangular with MDF=18mm Rectangular with MDF=18mm, internal air Rectangular with RW=18mm, internal air	
Model 6	Figure 22.f)	Circular with MDF=18mm Circular with MDF=18mm, internal air Circular with MDF=18mm, internal air	
Model 7	Figure 22.a)	Rectangular	Furnace
Model 8	Figure 22.b)	Rectangular with 36 mm of MDF	
Model 9	Figure 22.c)	Circular	
Model 10	Figure 22.d)	Circular with 36 mm of MDF	
Model 11	Figure 22.e)	Rectangular with 18 mm of MDF	
Model 12	Figure 22.f)	Circular with 18 mm of MDF	

5.3.2 Mesh and boundary conditions

A 2D finite element (Plane77) with 8 nodes was used for thermal and nonlinear material in transient analysis, using ANSYS© program. In order to fully satisfy the nonlinear conditions of the numerical problem, an iterative procedure in each time step it is necessary to apply. Figure 23 presents the correspondent mesh used in some models.

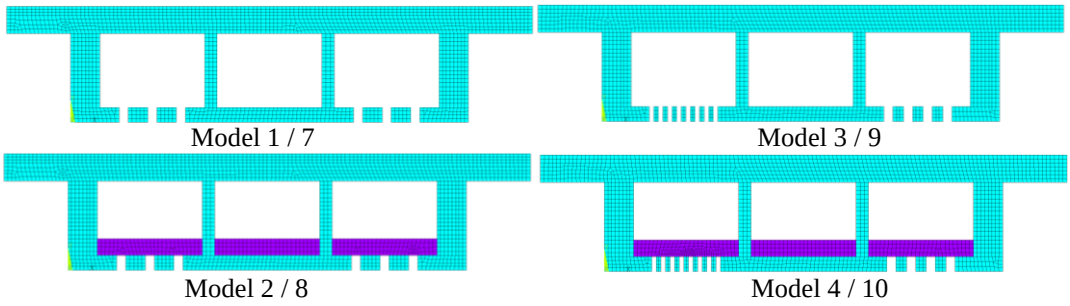

Figure 23- Mesh of finite element, plane77.

In ANSYS©, a modified Newton-Raphson method was adopted to solve the nonlinear problem, and the time interval considered for each step was equal to 10[s] and the minimum time equal to 0.1[s]. The bottom surface of the wooden slab was exposed to the boundary conditions according table 8 during 1800[s].

In wooden slabs without insulation material, the temperature on the internal cavities follows real heating curves obtained during the previous experimental tests, [27], [30], and measured with plate thermocouples. Figure 24 shows the values of each curve applied according the cell (TP1, TP2, TP3) and according the perforation type (rectangle or circle).

The convection coefficient is considered equal to 25[W/m^{2}K] [16] inside cavities and in the exposed fire surface. At the unexposed surface the room temperature is equal to 20[ºC] and the convection coefficient is equal to 4[W/m^{2}K]. The emissivity of the flames is taken equal to 1 for exposed side and internal cavities [16] and 0.8 for timber, according to Eurocode 5, [15]. The model with insulation material, all the adjacent cellular zones was filled with internal air, and only the conduction effect was considered.

Figure 25 gives the necessary curves of the temperature due the fire exposure, according the experimental tests in each type of slab ‘’Furnace’’ or using the ISO 834. These

curves were used in the numerical simulations. The ‘’Furnace’’ curve represents the increase temperature and the cooling effect during all experimental tests. This curve is more energetic due the conditions imposed by the space volumetric furnace and also due the wood material combustion.

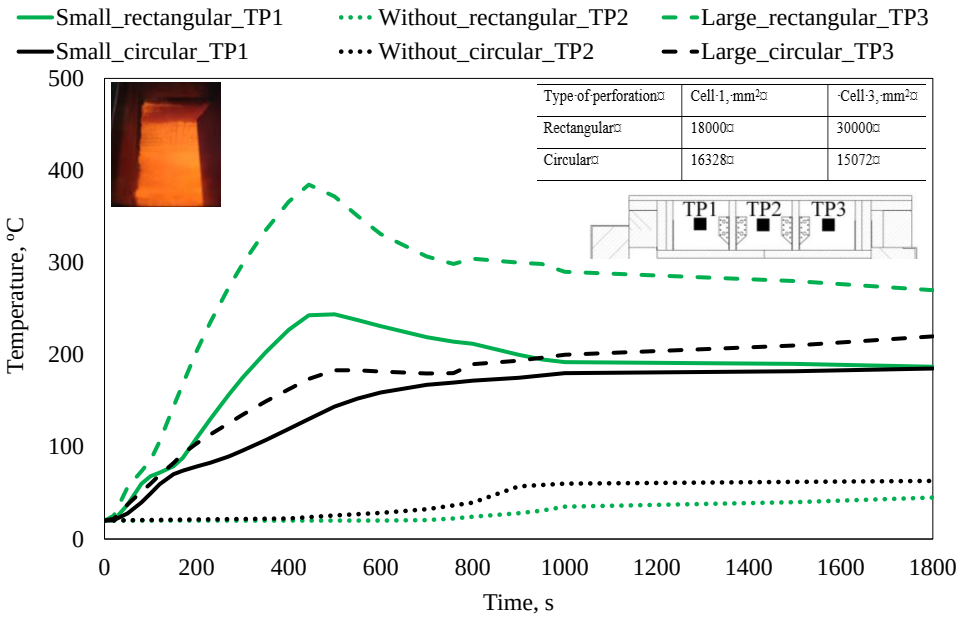

Figure 24- Temperature curves used inside the cavities in numerical analysis.

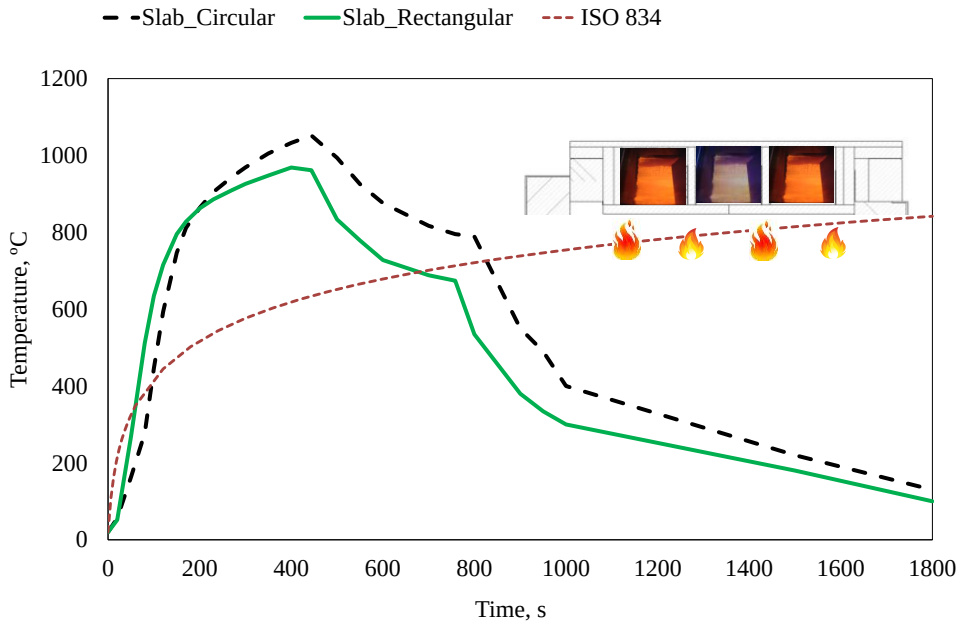

Figure 25- Curves of fire exposure ‘’Furnace’’ and ISO 834.

5.3.3 Results of 2D models

5.3.3.1 Charring rate

For the calculation of the charring rate by the numerical method, the criterion adopted was to calculated the isothermal at 300[ºC], determining the time instant that occurrence and calculate the developed char layer for each model.

The temperature limit at which it is estimated that the timber is completely carbonized is 300[°C], [15]. The timber which is at a temperature above this value is fully carbonized, below this temperature the wood is still intact. Firstly, it is necessary to know the value of the char layer for each model. The table below shows the thickness of char layer for each model with the considered time instant.

Table 9: Char layer depth.

Models	Time (s)	Cell 1 [mm]	Time (s)	Cell 2 [mm]	Time (s)	Cell 3 [mm]
Model 1	604.752	9	604.752	8	604.752	9
Model 2	630.062	9	716.663	8	630.062	9
Model 3	--	--	774.732	9	389.732	9
Model 4	--	--	784.967	9	404.967	9
Model 5	640	9	770	8	640	9
Model 6	--	--	784.586	9	399.586	9
Model 7	286.972	9	331.97	9	286.972	9
Model 8	300.428	9	330.428	8	300.428	9
Model 9	--	--	320.809	9	--	--
Model 10	--	--	300.862	8	230.699	8
Model 11	292.622	9	327.662	9	292.662	9
Model 12	--	--	332.427	9	--	--

The charring rate is calculated in cell 1, cell 2 and cell 3. The calculation was made using the equation 15 presented in Chapter 3. The values indicated are the average speed of carbonization for each of the three cells of the numerical model.

For circular models with and without MDF only the charring rate in cell 2 and cell 3 in some models were calculated. For cell 1 the perforations are totally charred at this time instant and for this reason it was not calculated.

There are typical design values for charring rate of wood between 0.5-1.0[mm/min]. Eurocode 5 [15] suggests a charring rate equal to 0.65[mm/min] for solid wood with density greater than 290[kg/m^3]. The evaluation of the char layer thickness depends on the exposed time and determines the charring rate in mm/min, shown in the table 10. The values are approximately equal to the reference value of EC 5 part 1.2, [15]. Cell 2 in all tested wooden slabs has a mean value equal to 0.71mm/min. On the other hand, in cell 1 and 3, the charring rates values are higher, due to perforations and their round effect. For models with ‘’Furnace’’ the results were compared with the results obtained previously from David and Meireles, [27], [30]. The numerical results obtained showed that the value of charring rate reaches more than 1 [mm/min], as the same results obtained from David and Meireles, [27], [30].

Table 10: Charring rates values.

	Charring rate [mm/min]		
Models	**Cell 1**	**Cell 2**	**Cell 3**
Model 1	0.89	0.79	0.89
Model 2	1.04	0.67	1.04
Model 3	--	0.69	1.38
Model 4	--	0.68	1.33
Model 5	0.84	0.75	0.84
Model 6	--	0.68	1.35
Model 7	1.88	1.62	1.88
Model 8	1.8	1.63	1.80
Model 9	--	1.68	--
Model 10	--	1.59	2.08
Model 11	1.84	1.63	1.84
Model 12	--	1.62	--

5.3.3.2 Temperature and residual cross-section of 2D wooden cellular slabs

In this section different study cases are presented. The numerical results are given in figures 26 and 27 in which the influence of different insulation materials and perforations were considered.

Figure 26 and 27 represent the temperatures at one side of fire exposure (bottom surface) in wooden slab with and without insulation material (MDF, RW) at 400[s] and the end of 1800[s], and the correspondent mesh. The physical behaviour of the wooden slab is conditioned by the char layer formation. This phenomenon only was considered in the post processor of the results, according to the criterion of char layer applied by the isothermal of 300[°C], Eurocode 5 part 1.2 [15]. The charring depth depends of the insulation material and also depends on the time of fire exposure.

The results show the residual cross section on the wood material, and the char layer in grey colour. According to the numerical results, the residual cross-section was concluded. The cellular zone without perforations has similar behaviour in all wooden slabs. At the end of fire exposure and inside these cells, temperatures are below than 100[ºC]. The cells with perforations don't have the same behaviour, all cross sections suffer high level of char due fire. At the last time instant of fire exposure the cells with perforations don't present any residual cross section. At time 400s, cell with small circular perforations anticipates degradation when compared with rectangular and higher circular perforations. Also the temperature at 400s and the end of fire exposure (1800s), each model follows the typical boundary condition used "Furnace" and the ISO 834 fire curve. The border of the rectangular and circular perforations present higher temperature when following the ISO834 fire event. Inside walls of the wood material the temperature remains small, [1], [44].

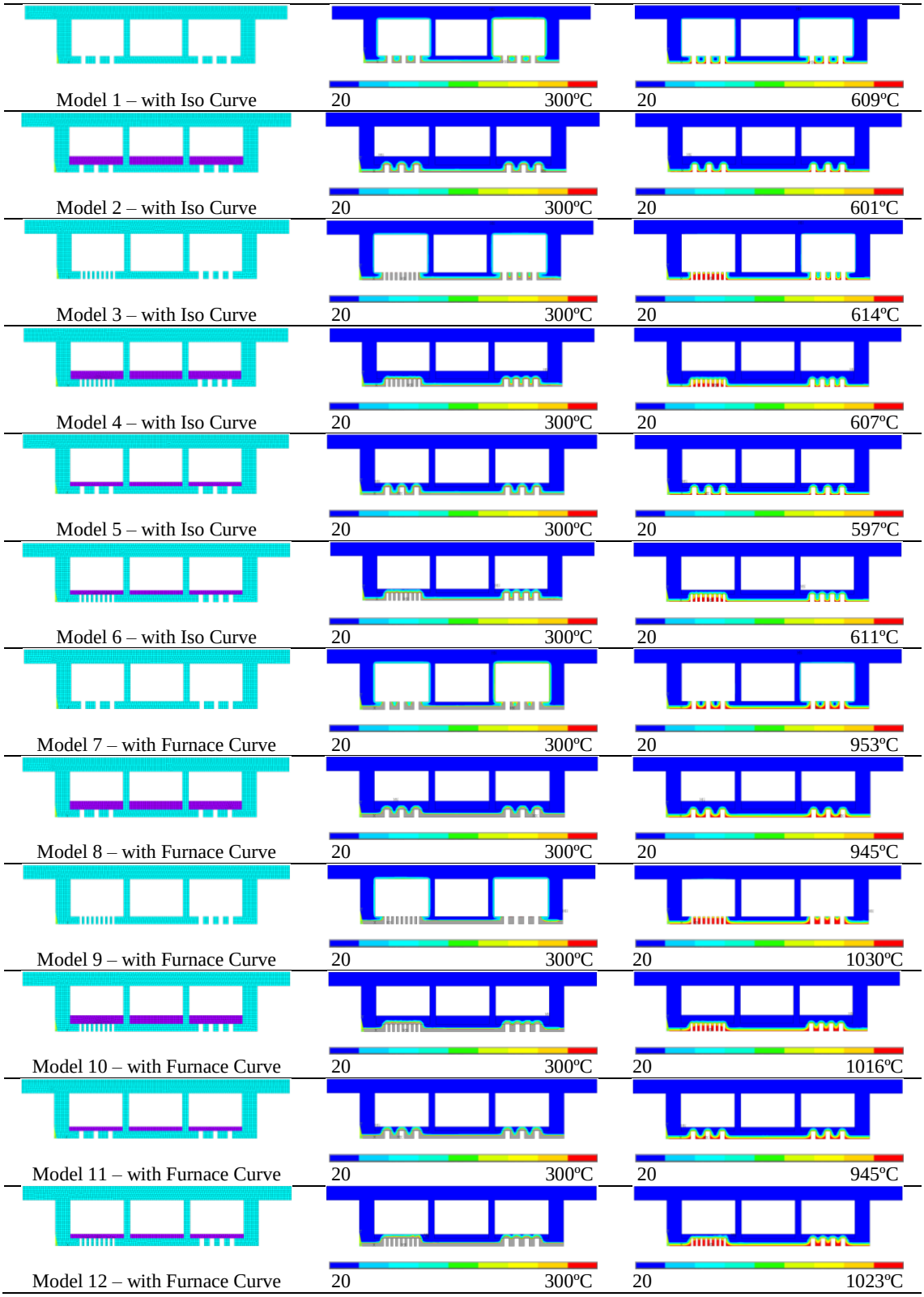

Figure 26- Temperature and residual cross-section of slab using MDF, at 400s.

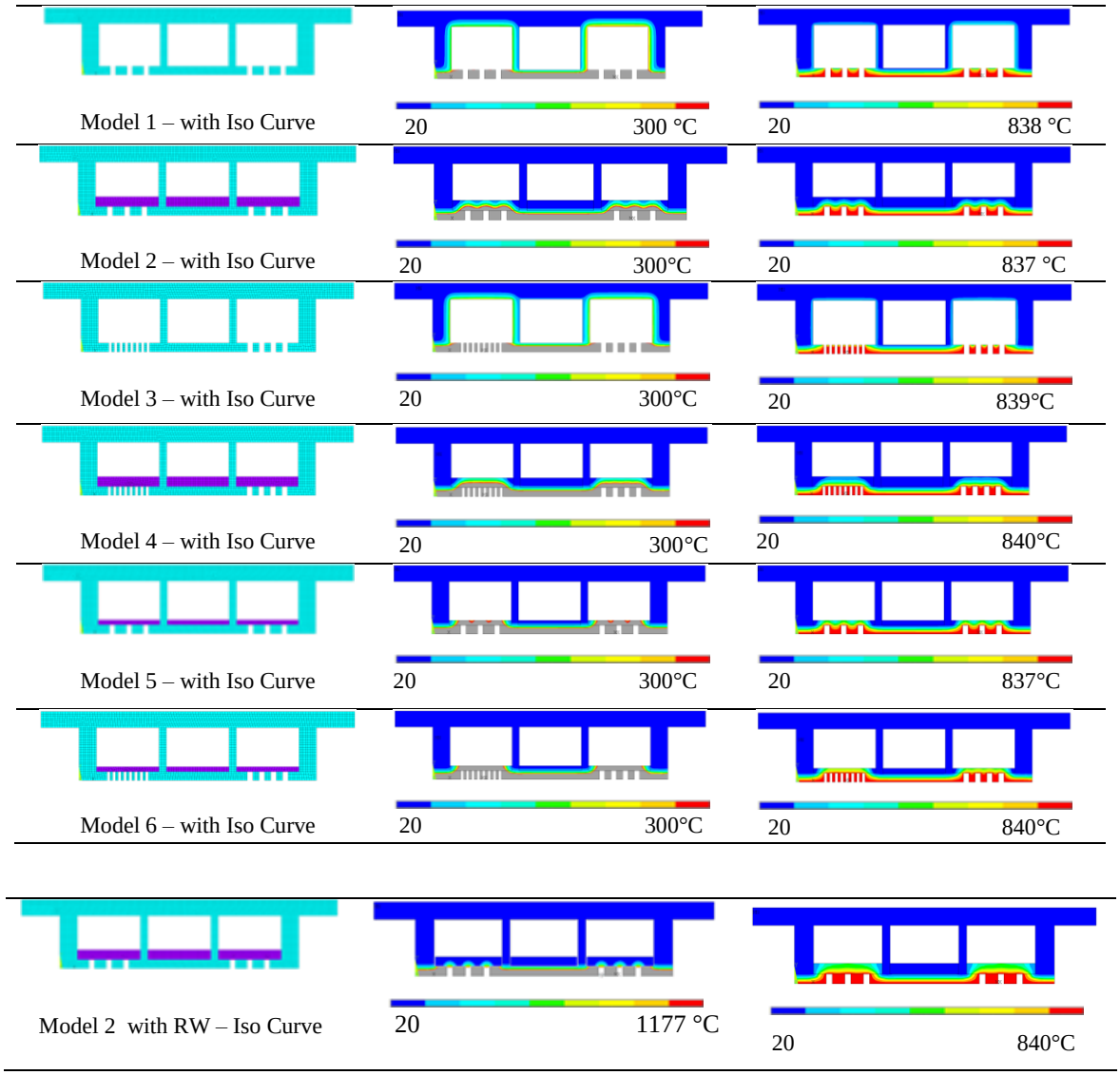

Figure 27- Temperature evolution and residual cross-section of slab using MDF, at 1800s.

The use of insulation material increases the fire resistance and the safety of the wooden slab, with no heat flow propagation for inside the cavities, until their degradation.

Figure 28 shows the temperature results obtained for the comparison between RW and MDF at 1800[s] of fire exposure. The use of RW material predicts high values of temperatures and allows the evolution of the heating process inside cavity due the value of thermal diffusivity of the material. Unlike when MDF material is used, the heat inside cavity is small due the thermal diffusivity of this material and the higher value of the density.

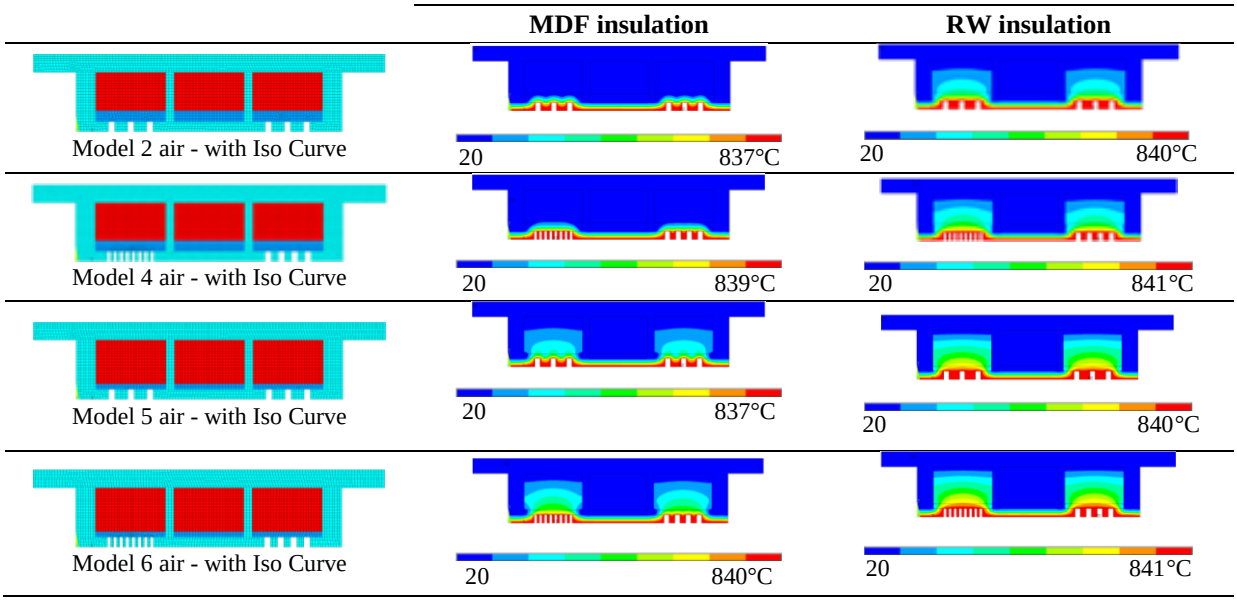

Figure 28- Comparison of temperature distribution between RW and MDF, time 1800s.

Figure 29 represents the comparison of residual cross-section in the previous models with internal insulation material (RW and MDF).

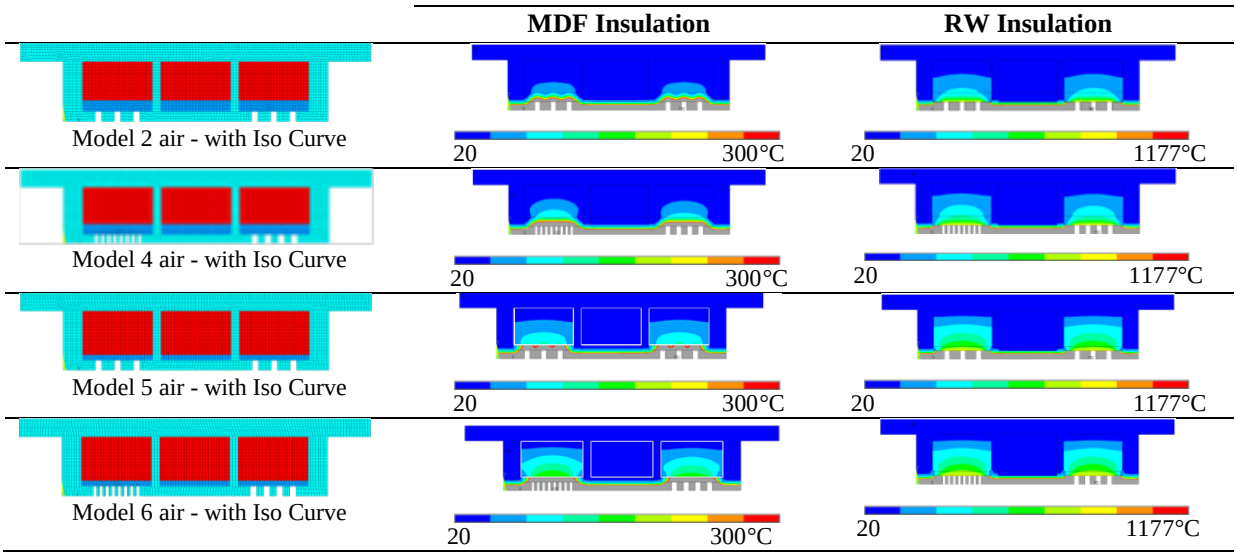

Figure 29- Residual cross-section of wooden slab with perforations with RW and MDF.

Results in figure 29 showed that the physical degradation for RW only starts when temperature reaches 1177[ºC]. Compared with MDF only resists until 300[ºC]. Two different thickness of insulation material were used. During the fire exposure of RW material resists without any degradation presenting more durability. MDF only resists when a board thickness is equal to 36[mm] in the model with rectangular perforations, [1], [44].

5.3.3.3 Time-temperature history in 2D wooden cellular slabs

The time temperature history was compared for each wooden slab when the insulation was changed (material type and size board), for different nodal positions and each cavity (1, 2, 3) during 1800[s] as represented in all models. The nodal positions were located in the border of the open zones, inside the cavities near of the wooden wall, and inside the cavities in the intermediate space. The nodal positions are placed always in the same positions in all slabs, as represented in all graphics. The numerical results were compared between all models, using the ISO 834 (I) or Furnaces (F) curves.

In figure 30 it was observed that in the border of the circular and rectangular perforation have higher values of temperatures when compared with all other nodal positions which remain at lower temperatures. It is possible to observe the evolution of temperature through all the event and the difference between the models with different perforations. In the rectangular model the evolution of temperature is approximately equal for cell 1 and 3, due to the existence of the same open space for the perforation. In cell 2 the evolution of temperature is smaller because there is any type of perforation. Also the same conclusions for rectangular model with MDF material were obtained. In case of the use of external furnace, the temperature increases until switch off the test furnace (410-450[s]) and decreases after this time. The use of ISO 834 fire curve is always increasing through all time of analysis. The temperature evolution for circular perforation is little higher in cell 3 when compared with cell 1 for model 3 and 9, unlike models with MDF the cell 1 and 3 are approximately equal. The mesh of this model could be more discrete, and improve better the results. The used meshes in all models are always regular and automatically generated with the same element length, equal to 9[mm]. Smaller dimension of the finite element could produces better nodal temperature results, due the neighbour location of their internal Gauss points.

In general, it can be concluded for all 2D models with rectangular perforations allow a fast heating process at higher temperatures compared to the circular perforations, [1], [44].

.

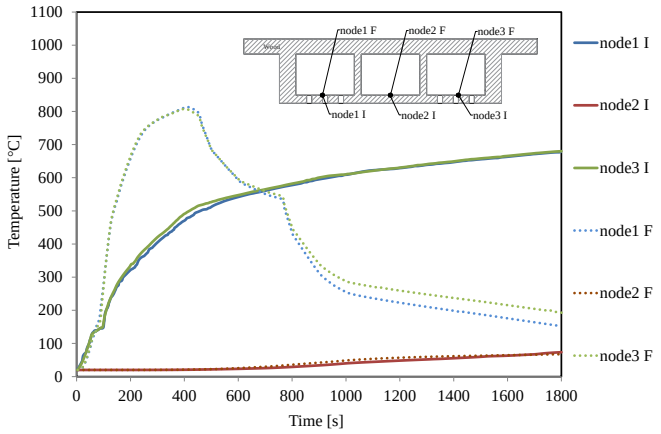

Model 1 and Model 7

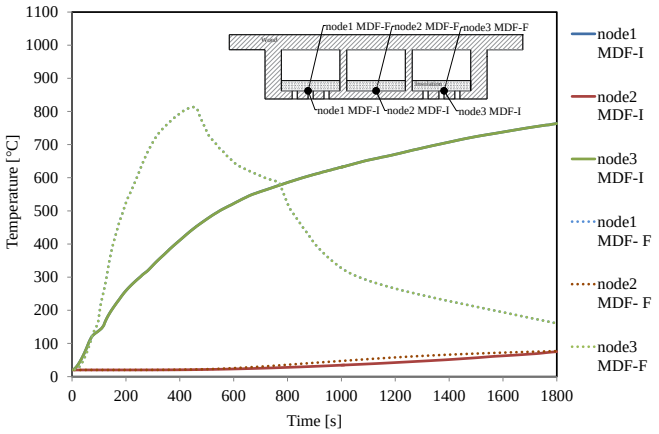

Model 2 and Model 8

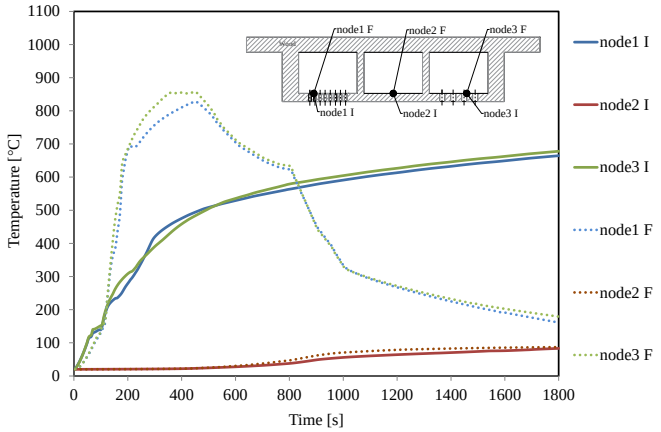

Model 3 and Model 9

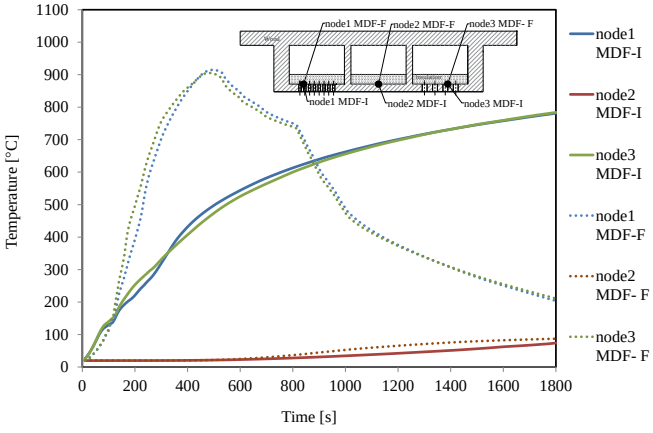

Model 4 and Model 10

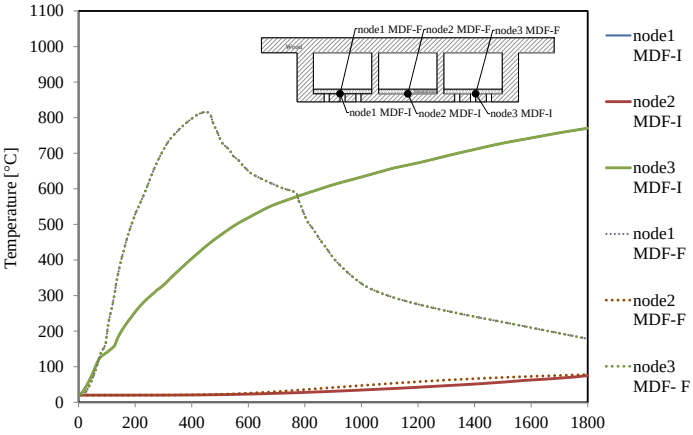

Model 5 and Model 11

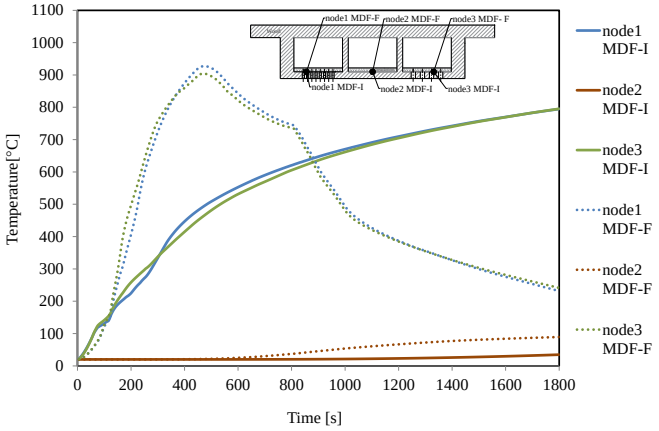

Model 6 and Model 12

Figure 30- Time-temperature in wooden slabs for models with ‘’Furnace’’ and ISO 834 curves.

Figure 31 represents the temperature evolution inside of the wooden wall in the neighbourhood of the board insulation. The insulation material has a greater effect for the evolution of temperature in all slabs. The time temperature history is very low curves when

compared with slabs without MDF slab 1/7 or 3/9. The MDF prevents the heat penetration inside the cavities. The evolution of temperatures for all cells is approximately equal. Nevertheless these nodal positions are not influenced by the external fire conditions, only influenced by the internal heating.

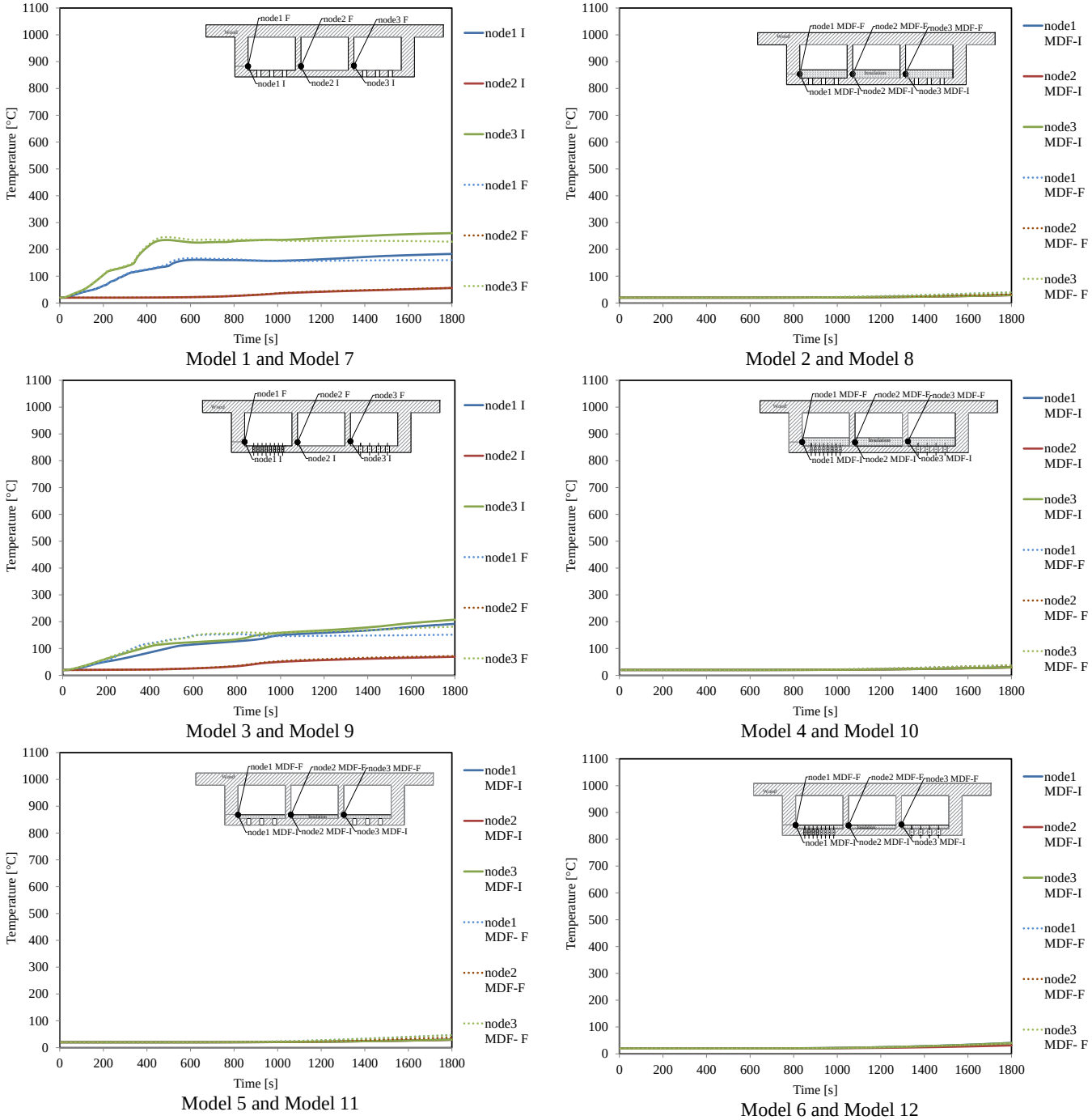

Figure 31- Time-temperature in wooden slabs with and without MDF.

Figure 32 represents the models analysed introducing internal air (A) inside the cavities, to compare the temperature evolution with numerical models without air, in some nodal positions in the neighbourhood of the board insulation.

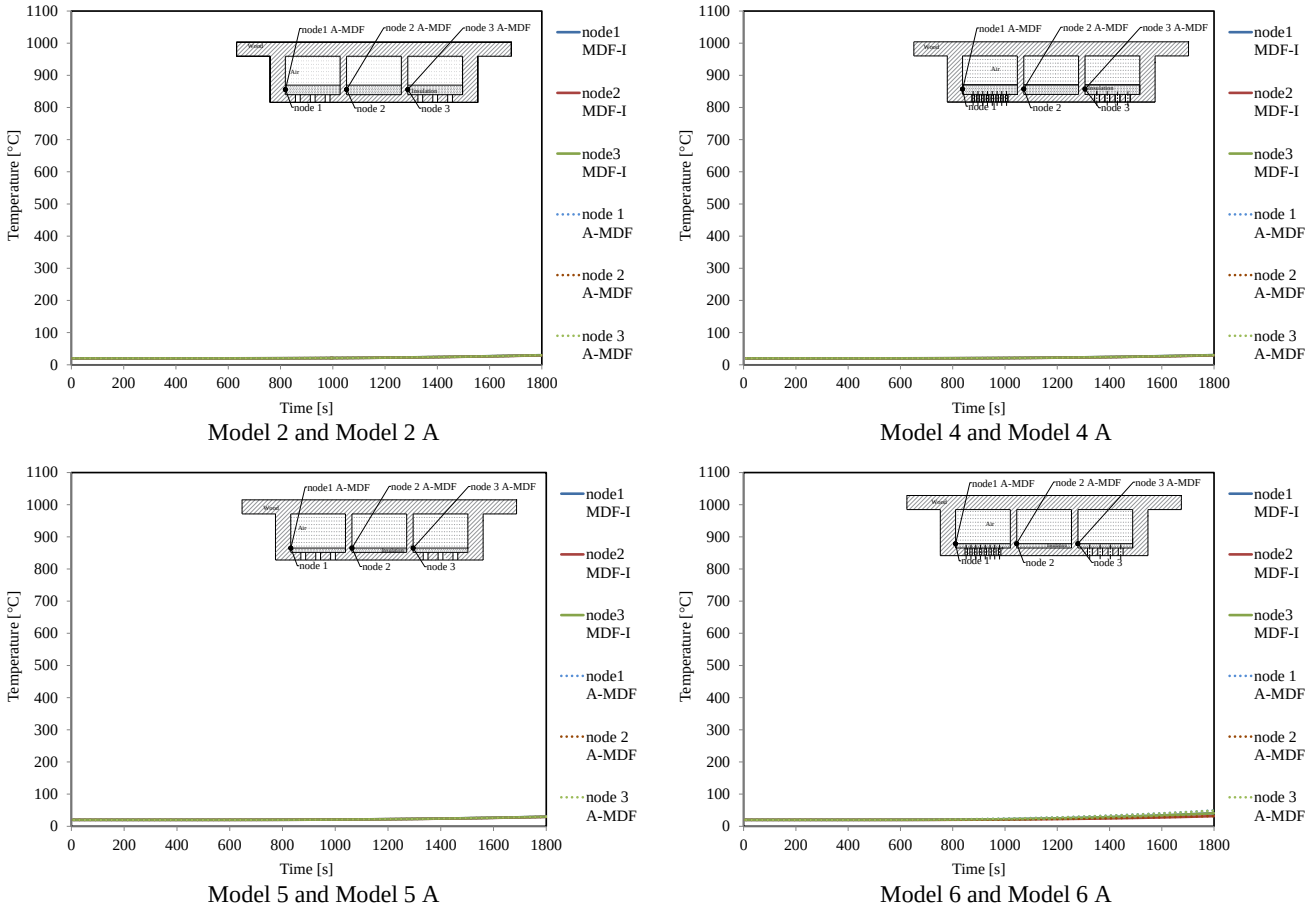

Model 2 and Model 2 A

Model 4 and Model 4 A

Model 5 and Model 5 A

Model 6 and Model 6 A

Figure 32- Time-temperature in wooden slabs in models with and without air.

According to the obtained curves, the evolution of temperature in models with and without air is approximately equal in all cells (1, 2, 3). It is concluded that modelling state air has no influence on the evolution of the temperature in this locations of nodal positions. But comparing the temperature in the postprocessor between all models, it is possible to understand the conduction of temperature inside the perforated cavities when the models were filled with internal air.

Also the time-temperature history for each wooden slab was compared between the results when the insulation was changed in material and board thickness.

Figure 33 and 34 show some graphs with the time-temperature history, in the perforated cells considering for comparison the same nodal positions in air mesh location (A) and in the corner of open space.

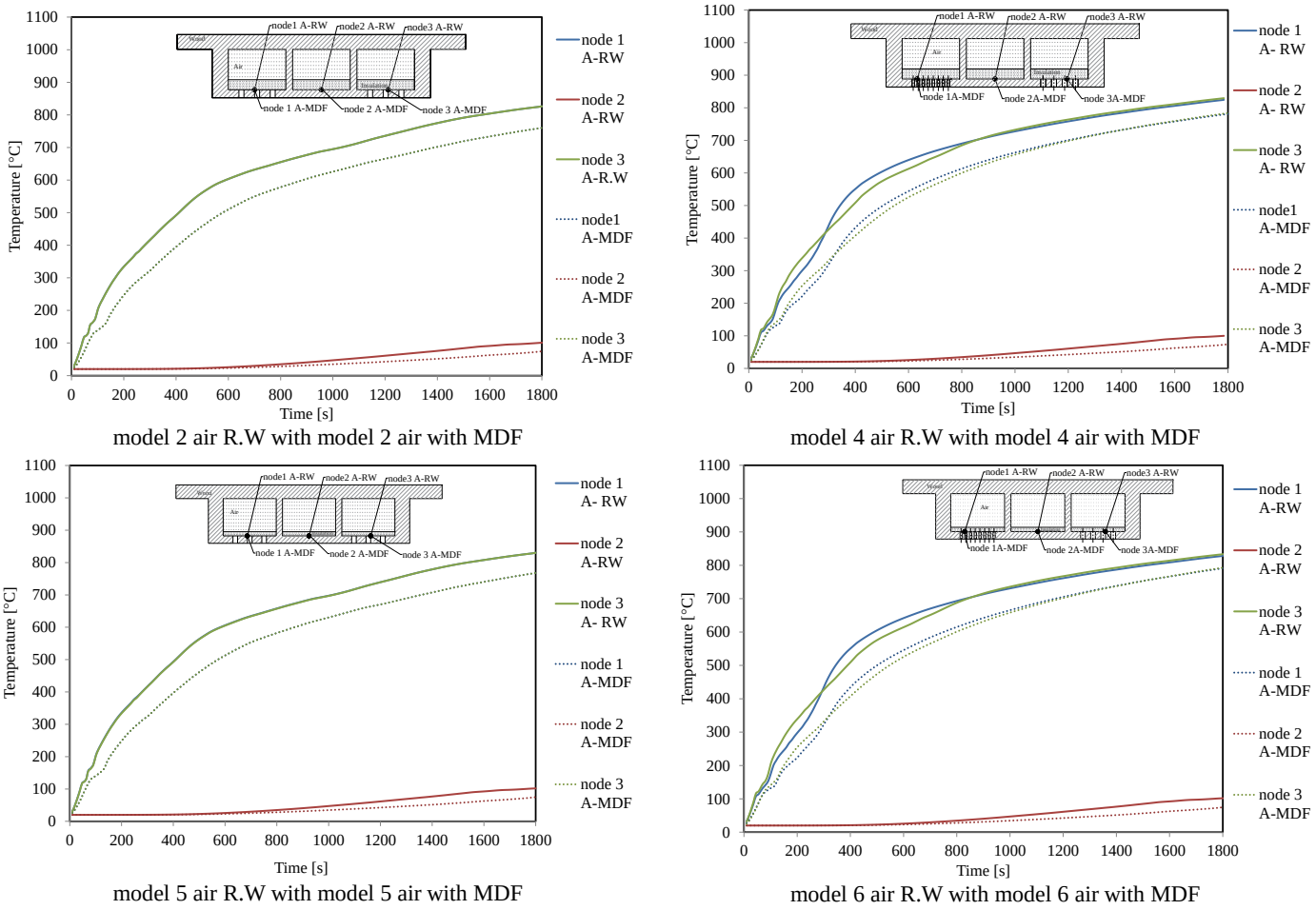

Figure 33- Time-temperature in wooden slabs in models with RW and MDF with air.

Figures 33 and 34 present the results between different insulation materials, MDF and RW, with different thickness, to determine the temperature evolution in different nodal positions. In general, the results show that the use of MDF produces lower temperatures than the use of RW insulation. In figure 33, in all nodal positions for cell 1 and 3 the temperatures follow the external fire condition, with a little increase in relation to the use of RW. In cell 2 always the temperature remains lower independently of the insulation material.

As a conclusion for results in figure 34, when the thickness of the insulation increases, the temperature evolution inside the cellular zones have a reduction on temperature

approximately equal to 100[ºC] at the end of the instant time. Also, the number and the dimensions of the circular perforations influences the temperature evolution between nodes. In the cellular zone with more perforations (even with lesser size) the heat flow is higher when compared with the cellular zone with lesser circular perforations. Time temperature history inside the cellular zones in the wooden slab with rectangular perforations depends on the insulation and the thickness size of the insulation material. The use of RW inside the cavities produces higher temperature evolution when compared with the MDF material. Also, the increase of the insulation thickness produces a decrease in time-temperature history inside the cavities, approximately equal to 100[ºC] at the end of the fire exposure time. In this wooden slab, the cavities have the same type of rectangular perforations and the temperature evolution has the same behaviour [1], [44].

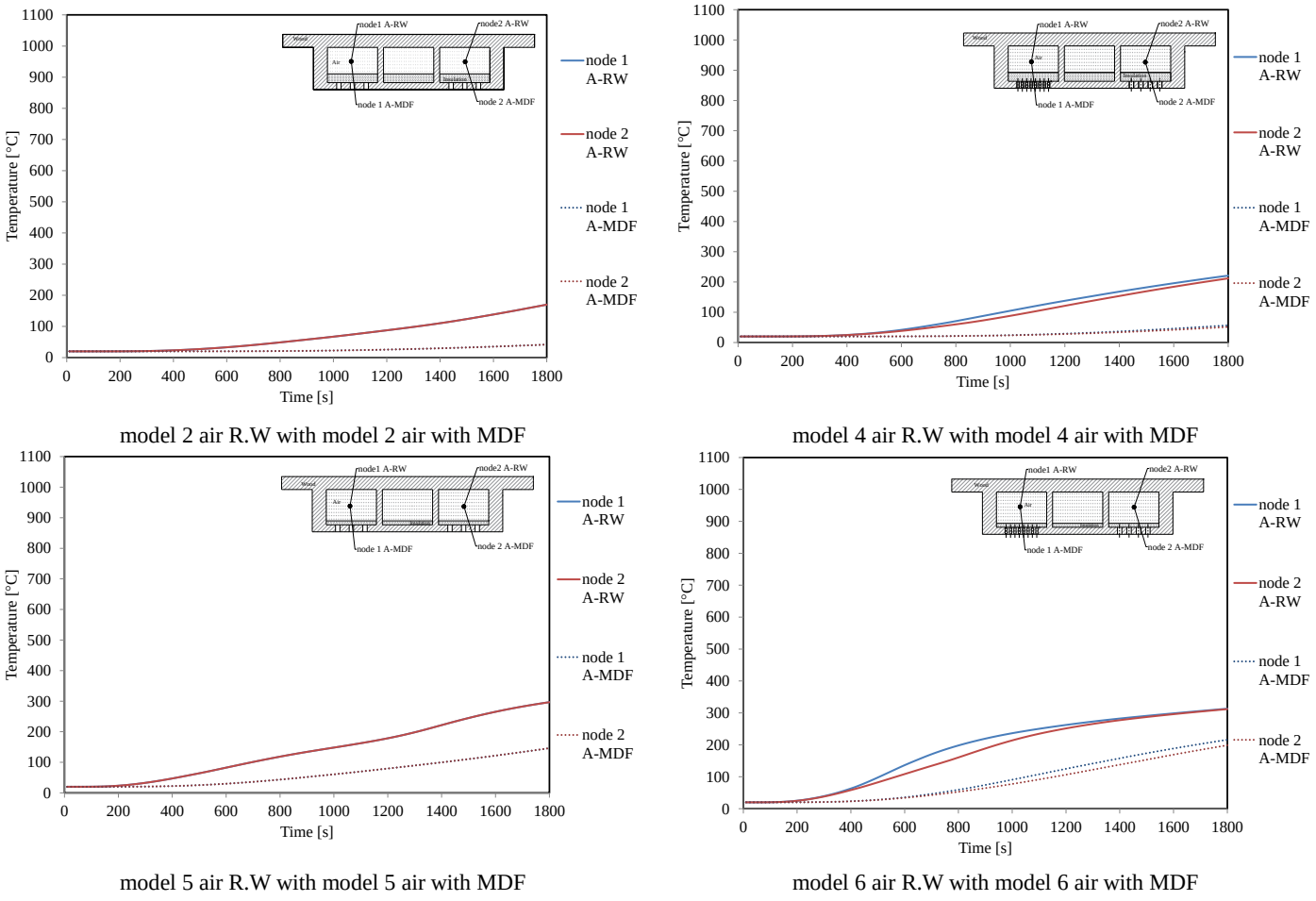

Figure 34- Time-temperature in wooden slabs.

5.4 3D Cellular slabs with perforations

5.4.1 Presentation of models and geometry

The computational model presented in this section, is based in the finite element method for 3D simulation. As referred, this method is much used to solve different mechanical problems, but also used to solve thermal problems. In thermal analysis the main objective is to determine temperature fields, as a useful tool for the analysis and verification of safety and structural stability.

ANSYS© program was chosen for this type of simulations, which will allow the analysis and verification of fire resistance. The first step is to build the model, using representative dimensions of typical slabs.

The proposed 3D model is only representative of the best studied 2D model, according the dimensions used previous [27]. This model has rectangular perforations, and also different insulation material (RW or MDF) for a thickness equal to 36mm. For this situation, only the perforated cavities were considered.

Different numerical models were produced as represented in table 11, to study different combinations of the insulation material with the same board thickness.

Table 11: 3D models characterizations.

Models	Geometrics	Boundary Conditions
Model 1	Rectangular	ISO 834
Model 2	Rectangular with MDF=36mm	ISO 834
Model 3	Rectangular with RW=36mm	ISO 834

Figure 35 represents the geometrical model with the location of the two cells. Figure 36 represents the mesh model used in ANSYS© program.

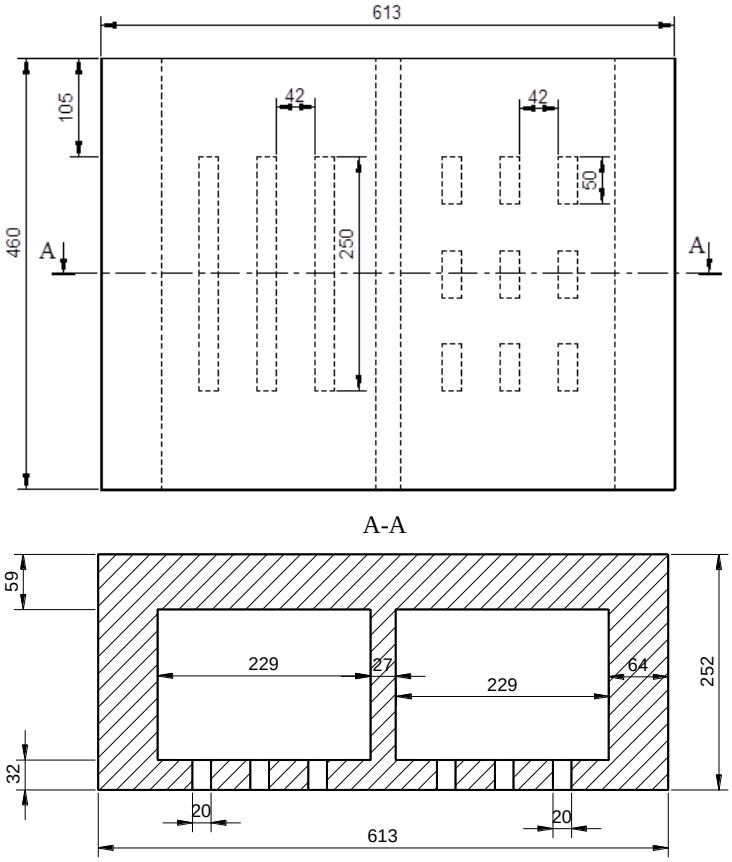

Figure 35- 3D model in Autocad.

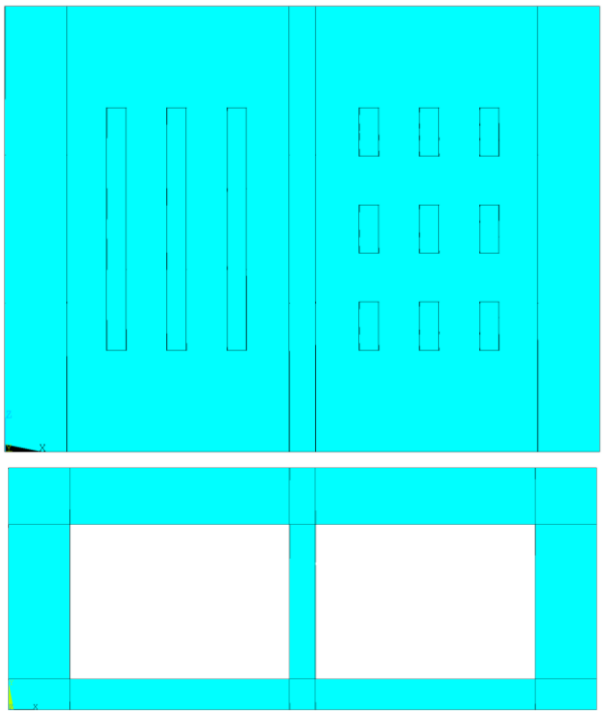

Figure 36- 3D model in Ansys program.

5.4.2 Mesh and boundary conditions

A 3D finite element (Solid90) with 20 nodes was used for thermal and nonlinear transient analysis, where each node has one degree of freedom, with a regular mesh using. Figure 37 represents the numeric model of the slab and the used mesh.

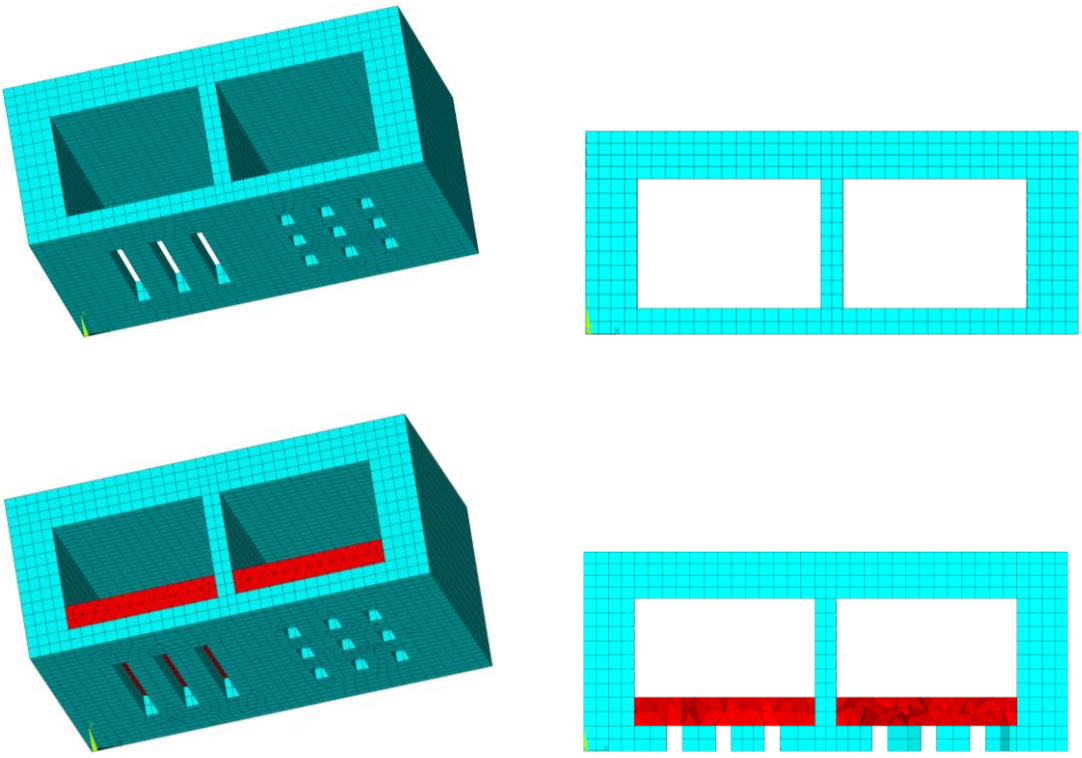

Figure 37- Mesh, solid elements with 20 nodes, with and without insulation.

The boundary conditions used in 3D model is the same as the boundary conditions used in 2D models. The convection coefficient is taken equal to 25[W/m^{2}K] [31] inside cavities and in the exposed surface. At the unexposed surface the room temperature (20[ºC]) is applied and the value of convection coefficient is equal to 4[W/m^{2}K]. The emissivity of the flames is taken equal to 1 for exposed side and internal cavities [16] and emissivity of 0.8 was considered for timber, according to Eurocode 5 part 1.2, [15].

5.4.3 Results of 3D models

5.4.3.1 Temperature evolution and charring layer for model 1

Figure 38 shows the temperature evolution at the end of fire exposure results representing the charring layer on the wood material, in grey colour. For the last time step the numerical results of 3D was compared with the 2D recorded, allowing to evaluate the residual cross section and the influence of different perforations on the fire resistance.

The wooden slab with higher perforations zone, represent a higher extension of damage. The rectangular perforations facilitate the heating process inside cavity and in the wall, compared with the squared perforations. It was observed also that the surface exposed to fire reaches higher temperatures. The charring layer is higher inside cavity with large perforations when compared with small perforations.

Higher temperature is affected in the cell with larger perforations for time equal to 400[s]

The numerical results of 3D are similar to the results obtained with the 2D models, and the charring depth depends on the time of fire exposure. Also the 3D model permits to identify all different regions (inside or outside) at different levels of temperature in different views.

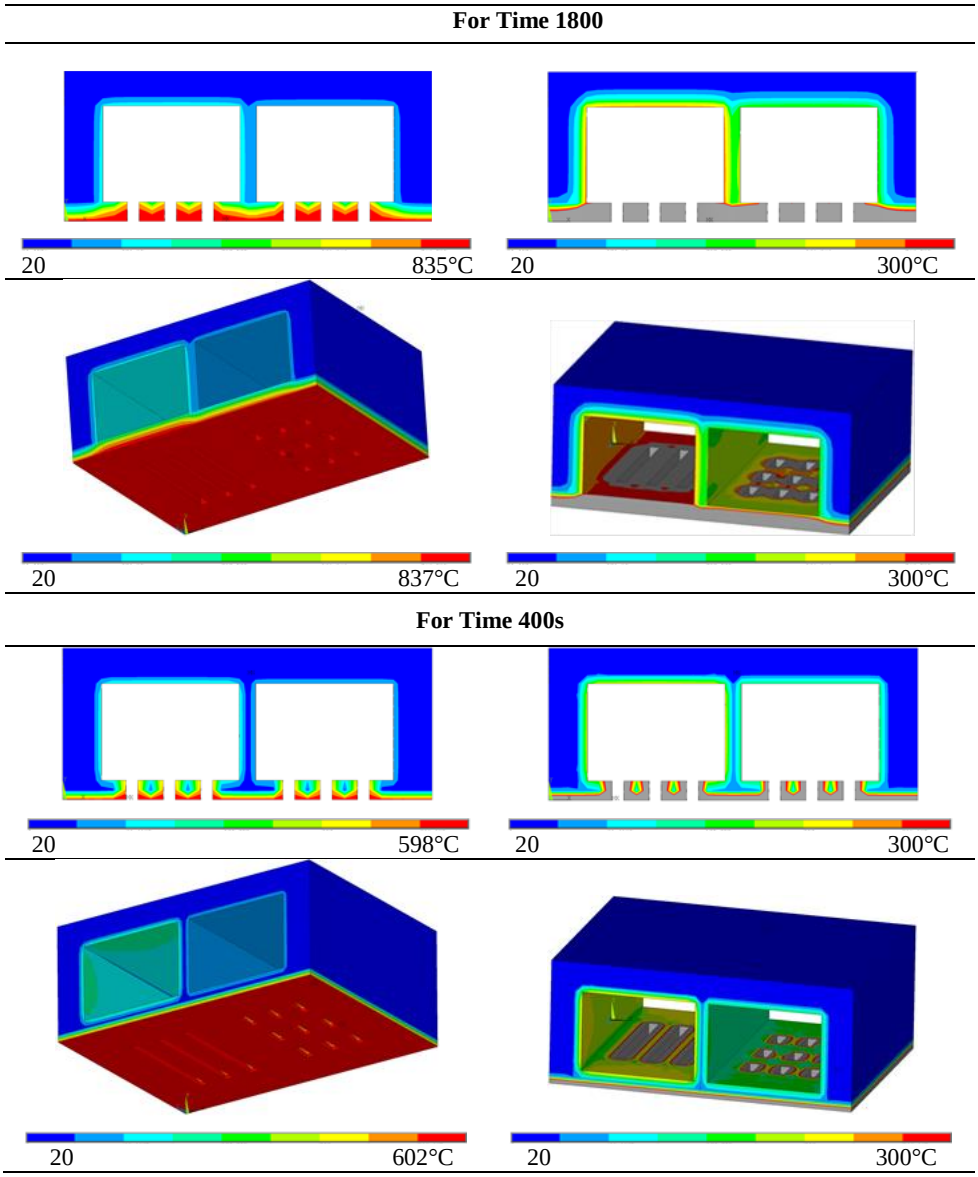

Figure 38- Temperature evolution and residual cross-section of 3D wooden slab.

5.4.3.2 Time-temperature history in 3D wooden cellular slabs model 1

The time temperature evolution of slab 3D was compared with 2D results, in particular for the same nodal positions during 1800[s].

Figure 39 represents the temperature evolution in different locations in the corner of the open spaces. The simulation gives the results obtained through the nodal points, presenting the profile of the temperatures on the face not exposed to fire. The results for 3D shows that the time temperature history is higher in cell with large perforations compared with small perforations. The comparison between 2D and 3D models are approximately in good

accordance. The obtained results continue to increase and follow ISO 834 curve. The differences between the 2D and 3D curves are very small, and derived from the time step size used in the numerical solution due to the convergence process.

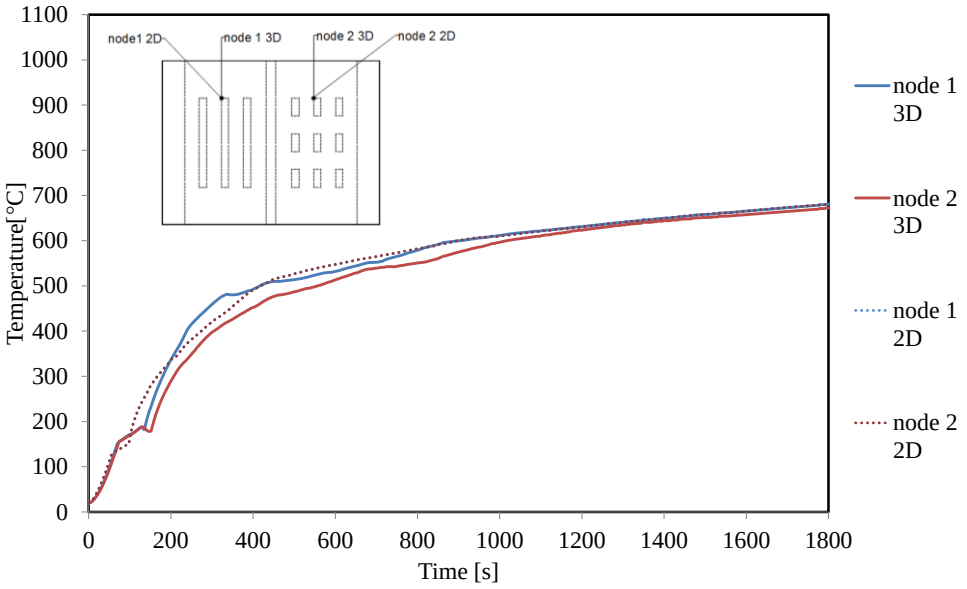

Figure 39- Time-temperature history in wooden cellular slab for models 2D and 3D.

5.4.3.3 Temperature evolution and charring layer for model 2

Figure 40 represents the temperature evolution at the end of fire exposure for cellular wooden slab with rectangular perforations using an additional insulation material MDF with size equal to 36[mm]. The charring layer on the wood material is presented below during different time instant in grey colour. The results were compared with the 2D model, allowing to evaluate the residual cross section and the influence of different perforations.

The results show that the use of insulation material increases the fire resistance of the wooden slabs, also prevents propagation of heat flow inside cavities due to high value of density for MDF and value of thermal diffusivity. But MDF material doesn't resist for high values of temperature, due the physical degradation starting at 300[°C].

Results for time 400[s] showed that the evolution of temperature is not higher inside cavities; also the charring layer is lower.

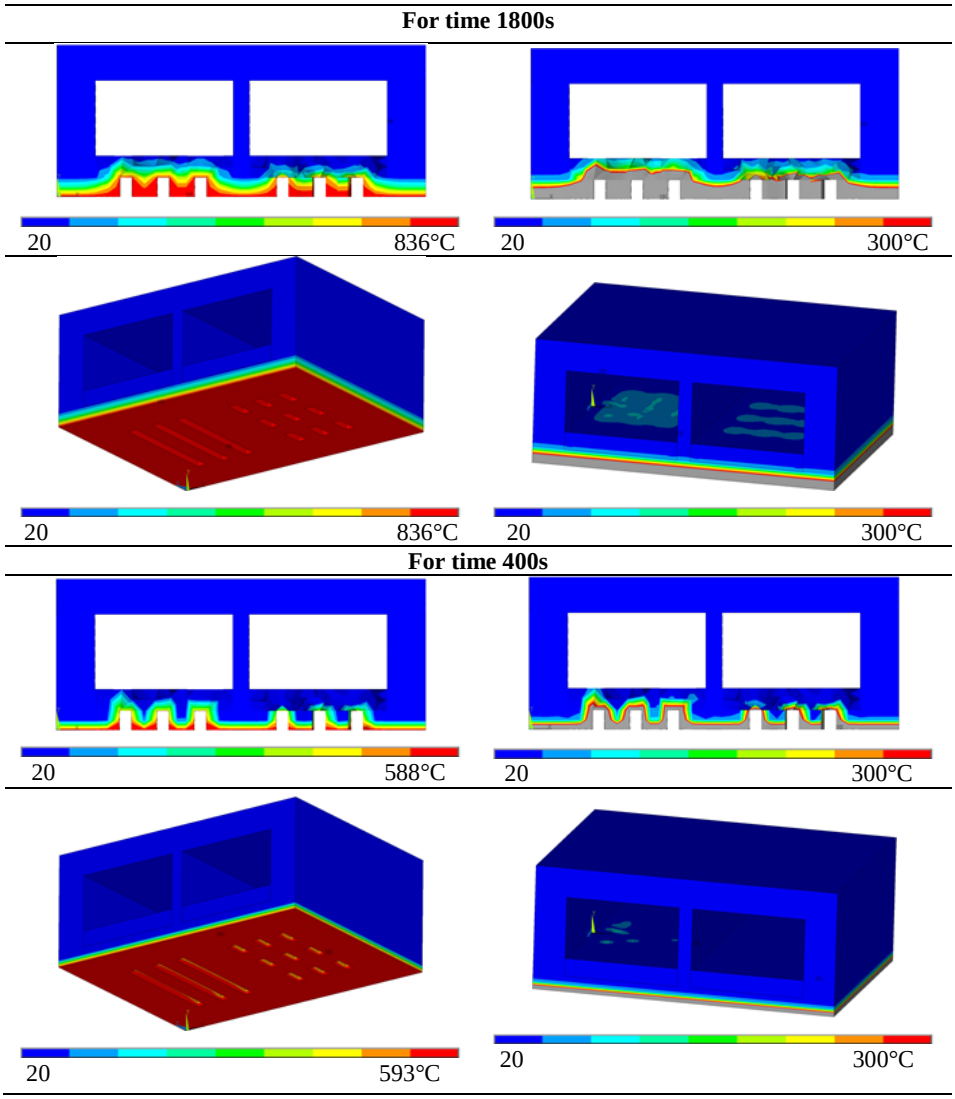

Figure 40- Temperature and residual cross-section of 3D wooden slab, MDF=36mm.

5.4.3.4 Time-temperature history in 3D wooden cellular slab model 2

The time temperature history was also compared in wooden slab with perforations in figure 41 using an additional insulation material MDF (36[mm]), with model 3D and 2D during 30[min] of fire exposure. The results obtained for 3D showed that the time temperature history is higher for cell with large perforations compared with cell with small perforations. As regards, the comparison between the time-temperature history for 3D results are in agreement with 2D results. Some discrepancies between both results may be justified due to

the mesh size. The length used for each finite element in 3D is different from the length used in 2D. In general, good agreement was found between both results.

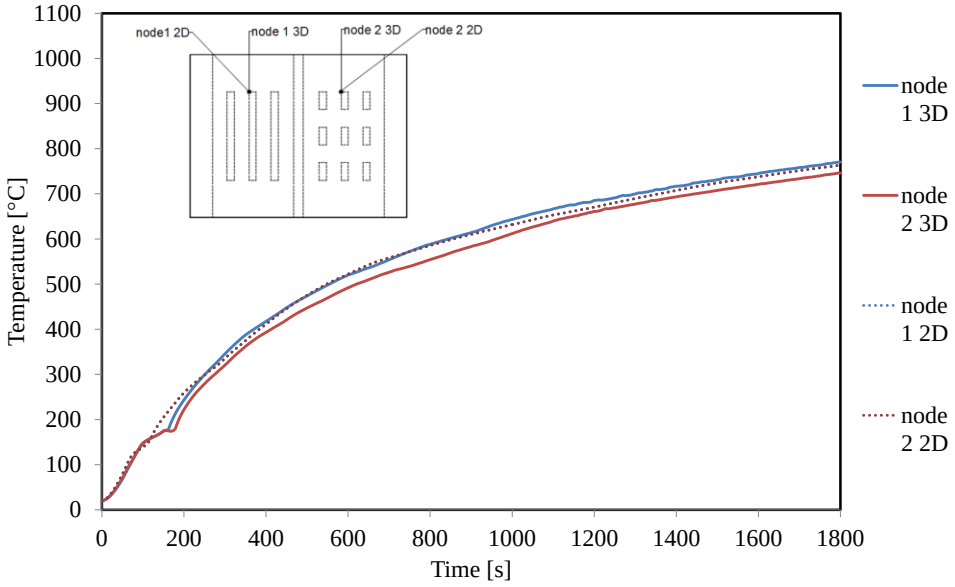

Figure 41- Time-temperature in 2D and 3D wooden slab with MDF.

5.4.3.5 Temperature evolution and charring layer for model 3

The temperature evolution at the end of fire exposure is represent in figure 42, for cellular wooden slab with rectangular perforation using an additional insulation material Rockwool (RW) with size equal to 36[mm]. The grey colour represents charring layer on the wood material. Also the results were compared with 2D slab, to evaluate the residual cross section and the influence of different perforations on the fire resistance. The results showed that the use of RW material offers high resistance. It was observed that the used RW enable the propagation of heat inside cavities due the diffusivity. Also RW material resists for high value of temperature and the degradation start only at 1177[°C]. The results obtained from 3D models confirmed results of 2D.

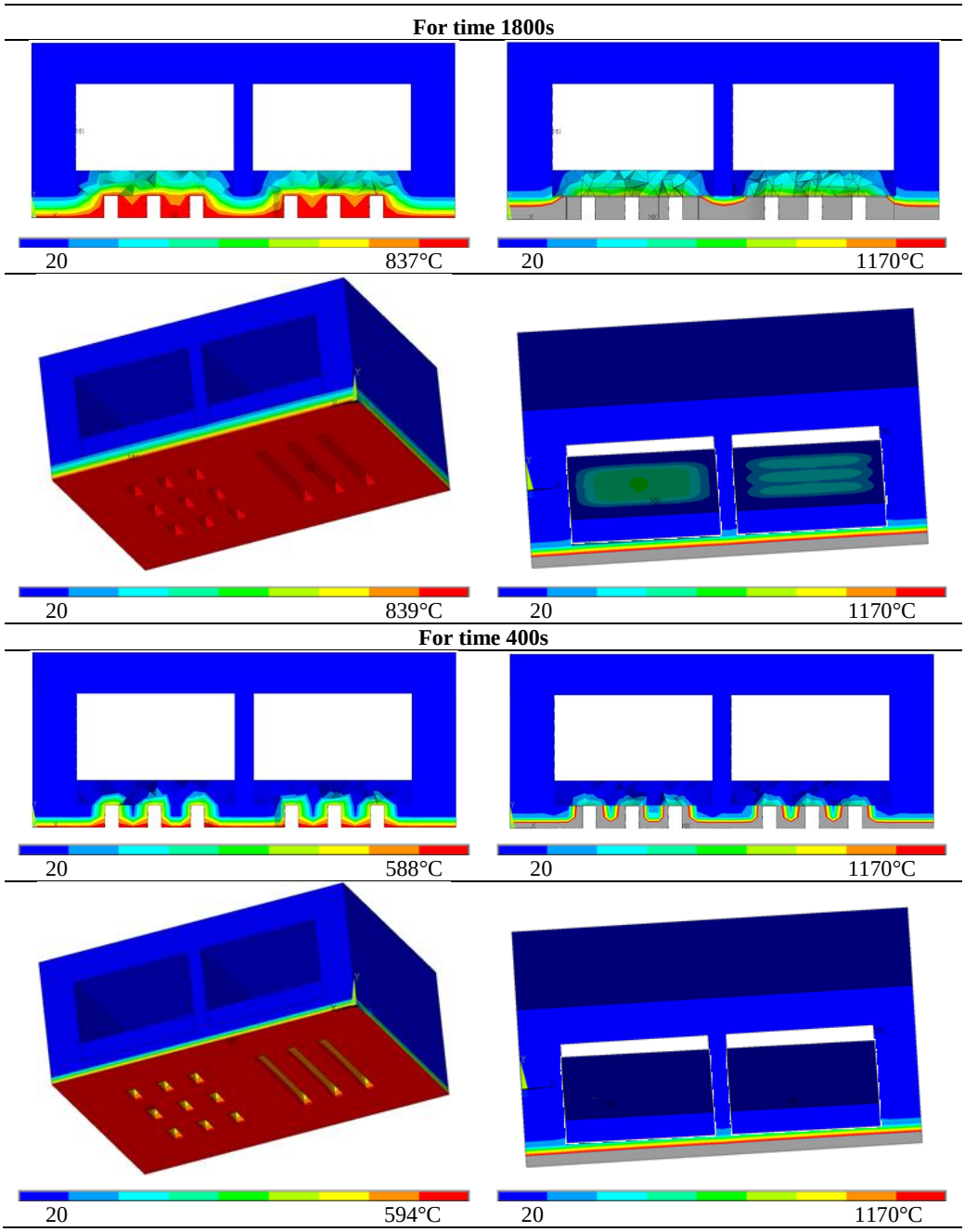

Figure 42- Temperature and residual cross-section of 3D wooden slab, RW =36mm.

5.4.3.6 Time-temperature history in 3D wooden cellular slab model 3

Figure 43 represents the comparison of time temperature history in wooden slab with perforations using an additional insulation material RW with 36[mm], between model 3D and 2D during 30[min]. The obtained results in 3D are very similar with results obtained in 2D. The models have the same behaviour, and also it was observed that the curves keep the same

difference, following ISO 834 curve. Similar conclusions can be point out, being the differences justified by the mesh and model (full 3D).

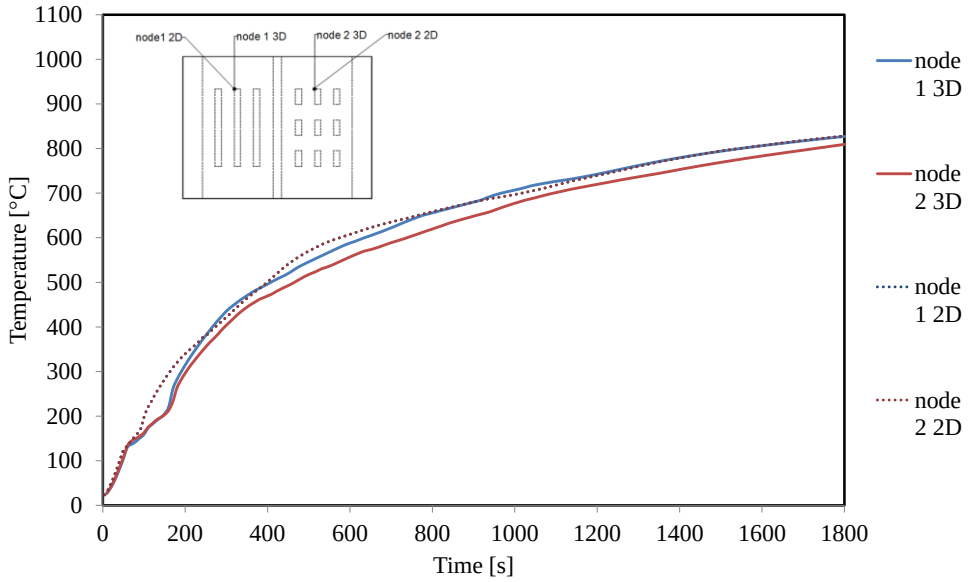

Figure 43- Time-temperature in 2D and 3D wooden slab with RW.

Chapter 6

Conclusions and Future Work

6 Conclusions and Future Work

The work presented reports numerical simulations of 2D and 3D models focus on thermal analysis in transient regime and nonlinear behaviour of material. The models represent wooden cellular slabs with different perforations on the ceiling plate of the slab, subject to fire situations using different insulations material, rockwool (RW) and medium density fibreboard (MDF), allowing to analyse the evolution of temperature, determine the char layer formation and the charring rate.

The comparison of several results obtained by 3D and 2D models showed a good accordance. These numerical simulations are very important, the models can be used for verification in other type of structures subjected to fire action.

Wood material when exposed to fire presents a thermal physical degradation. In wooden slab with perforations, the type and the size of perforation can limit the use of these constructive elements in terms of fire resistance. Also the different temperature evolution obtained, is due to the size of the perforations. The calculated charring rates are approximately equal to Eurocode 5 part 1.2 only for cell 2. Cell 1 and 3 is higher due to the perforations. These constructive elements should be chosen before, to prevent and delay the fire damage effect, allowing that the slab could remain in service with more safety and durability. Cells without perforations (cell 2) are more stable under fire conditions (45min), when compared with cells with perforations (cell 1 and 3) under the same condition (30min). Slab without perforations resists on average more 15[min].

The use of insulation material increases the fire resistance and the safety of the wooden slab, with no flames propagation to inside the cavities. The insulating materials are based on the thermal properties which include the density, low thermal conductivity and high specific heat. Also a lower thermal diffusivity leads to a good thermal insulation. This parameter determines the temperature distribution in non-steady or transient conditions and measures the ability of a material to reacts to fire, indicating how quickly a material's temperature will change. Increasing the thickness of the protection material, will reduce the temperature level inside the cellular zones, the temperature reduction is approximately to 100[°C for the last time of fire exposure. The use of RW enables the evolution of heating inside the cavities,

when compared with MDF. Also the temperature degradation of RW is higher (>1000[ºC]) when compared with MDF (300[ºC]).

Finally, the results showed in this work, reveal extreme importance because they give great information for designers, more details about the behaviour of the wooden structures and the use of insulation materials in simultaneous, in fire situations. This knowledge can be taken into account for the building construction to minimize the risk of collapse and increasing the safety of people.

Considering the works carried out in this study, some suggestions for future work will be presented as the following:

-carry out different experimental and numerical tests with other insulation materials (Gypsum board, Fibreglass) and using different sizes geometries;

-carry out the same numerical models but using the Ansys CFD (Computational Fluid Dynamics) solutions to give the power to model and simulate all fluid process inside cavity (fluid-structure multiphysics interactions);

-carry out a numerical study using steel connections in the wooden slabs under fire conditions.

Chapter 7

Bibliography

7 Bibliography

[1] Djaafer Haddad, Elza M. M. Fonseca and Belkacem Lamri; Thermal model for charring rate calculation in wooden cellular slabs under fire; 7th International Conference on Safety and Durability of Structures ICOSADOS 2016, 10-12 maio 2016, Proceedings in Pen USB flash drive ISBN:978-989-20-6683-7, Vila Real, Portugal 2016.

[2] Frangi A., Fontana M. Fire behaviour of timber surfaces with perforations, Fire and Materials, vol.29, 2005, p. 127-146.

[3] Janssens M.L. Modeling of the thermal degradation of structural wood members exposed to fire, Second International Workshop ‘’Structures in Fire, vol. 28, 2001, p. 211-222.

[4] Frangi A., et al. Charring model for timber flame floor assemblies with void cavities, Fire Safety Journal, vol.43, 2008, p. 551-564.

[5] Frangi A., Fontana M. Charring rates and temperature profiles of wood sections, Fire and Materials, vol.27, 2003, p.91-102.

[6] ISO 834-1. Fire resistance test - Elements of building construction. Part 1: General requirements. September de 1999.

[7] Cachim P.B., Franssen J.M. Assessment of Eurocode 5 Charring rate Calculation Methods, Fire Technology, vol. 46, 2010, p. 169-181.

[8] Fonseca E.M.M., Barreira L.M.S. Charring rate determination of wood pine profiles submitted to high temperatures. WIT Press, 3 Int. Conf. on Safety and Security Eng., vol.108, 2009, p. 449-457.

[9] Fonseca E.M.M., Barreira L.M.S. Experimental and Numerical Method for Determining Wood Char-Layer at High Temperatures due an Anaerobic Heating, Int. Jour. of Safety and Security Eng., vol.1(1), 2011, p. 65-76.

[10] Fonseca E.M.M., et al. Fire safety in perforated wooden slabs: a numerical approach, WIT Press, 5 Int. Conf. Safety and Security Eng., vol.134, 2013, p. 577-584.

[11] Fonseca E.M.M., et al. Numerical Model to Assess the Fire Behaviour of Cellular Wood Slabs with Drillings, 4 Int. Conf. on Integrity Reliability & Failure, S. Gomes et al (Eds.), 2013.

[12] Frangi A, Fontana M., Untersuchungen zum Brandverhalten von Holzdecken aus Hohlkastenelementen. Institut für Baustatik und Konstruktion, Zurich, 2004.

[13] David C., et al., Fire Resistance of Cellular Wooden Slabs with Rectangular and Circular Perforations; 6 Int. Conf. on Mech. and Materials in Design M2D, p. 2323-2330, Azores, 2015.

[14] David Couto, Elza Fonseca, Paulo Piloto, Jorge Meireles, Luísa Barreira, Débora Ferreira. Fire resistance of cellular wooden slab with rectangular and circular perforation, IFireSS – International Fire Safety Symposium Coimbra, Portugal, 20th-22nd April 2015.

[15] EN1995-1-2. 2003: Eurocode 5: Design of timber structures - Part 1-2: Structural fire design. Brussels, CEN, European Committee for Standardization, 2003

[16] EN1991-1-2, Eurocode1: Actions on structures -Part 1-2: General actions- Actions on structures exposed to fire, November de 2002.

[17] ASTME119, Standard Test Methods for Fire Tests of Building Construction and Materials, American Society for testing and Materials, 2008

[18] Brian Twomey, The performance and Behaviour of light weight wood exposed to fire condition, thesis of master in civil engineering, Faculty of Worcester Polytechnic Institute May 2007.

[19] Ari Vepsalainen, Janne Pitkanen, Timo Hyppanen, Fundamentals of heat transfer, page 179. ISBN 978-952-265-127-3, 2011.

[20] Barreira, Luísa Maria da Silva, Estudo Numérico do Comportamento Térmico e Mecânico de Estruturas em Madeira. Bragança IPB Instituto Politécnico de Bragança, 2008.

[21] Christong, Naser Sayma, Heat Transfer, ISBN 978-87-7681-432-8, 2009.

[22] Özisik, M. Necati, Transferência de calor, Um Texto Básico, Rio de Janeiro, RJ - CEP 230040-040, Guanabara Koogan,1990.

[23] Exemple of convection heat transfer, page used, https//www.tutorvista.com, 22/10/2015.

[24] Solid works help, https//solidworkes.com, Page used 22/10/2015.

[25] Luis Fernando, Martins Barbosa, Pedro Manuel, Loureiro de Almeida, Análise numérica de Estruturas em Madeira e/ou aço sob a ação de fogo, Relatório de Projeto em Engenharia Mecânica.

[26] Coelho. Diana Silva, Computational Model for Thermal and Mechanical Assessment of Timber Structures, thesis of Master, Bragança 2011.

[27] Jorge Manuel Meireles, Fire behaviour of cellular wood slabs with perforations thesis of master in Industrial Engineering 2014.

[28] Hélder José Gonçalves, Da Silva & Hugo Miguel Esteves Ramos, Análise de Estruturas em Aço e Aço/Madeira sob a ação do Fogo, Relatório de Projeto em Engenharia Mecânica, julho 2013.

[29] Barreira L. e Fonseca, E. M. M., Método experimental para determinação da espessura carbonizada na madeira quando submetida a altas temperaturas, Bragança, 2010.

[30] David Léandro Pinto do Couto Fire behaviour of cellular floor or roof wooden slabs with circular perforations. Thesis submitted to fulfil the requirements of Ms.C degree in: Industrial Engineering 2015.

[31] Janssens Marc, Modeling of the thermal degradation of structural Wood members exposed to fire, fire and materials volume 2B, 2004.

[32] Yuliati Indrayani, Dina Setyawati, Kenji Umemura & Tsuyoshi Yoshimura, Decay Resistance of Medium Density Fiberboard (MDF) Made from Pineapple Leaf Fiber, Faculty of Forestry, Tanjungpura University, Jalan Imam Bonjol, Pontianak 78124, Indonesia Research Institute for Sustainable Humanosphere (RISH), Kyoto University, Uji, Kyoto 611-0011, Japan, J. Math. Fund. Sci. Vol. 47, No. 1, 76-83, 2015.

[33] ISO TC 163/SC 2:2007. Building materials and products - Hydrothermal properties, Tabulated design values and procedures for determining declared and design thermal values. Geneva: ISO, 2007.

[34] Bamboo Based Bio Composites Material, Design and Applications, https//www.intec hopen.com, page used 05/11/2015.

[35] Chaykovskiy German, Comparison of Thermal Insulation Materials for Building Envelopes of Multi-storey Buildings in Saint-Petersburg, Bachelor Thesis December 2010.

[36] Apache- Tables User Guide, IES Virtual Environment 6.4

[37] The Engineering ToolBox, http://www.engineeringtoolbox.com/, Page used 19/01/2016.

[38] Shakhashiri, GASES OF THE AIR, chemical of the week, Chemistry 103-1, www.scifun.org, November 2007.

[39] Thermophysical properties of materials for nuclear engineering: a tutorial and collection of data, IAEA, VIENNA, 2008, IAEA-THPH, ISBN 978–92–0–106508–7, Printed by the IAEA in Austria, November 2008.

[40] G.P.Nikishkov, Introduction to the finite element method, University of Aizu, Aizu-Wakamatsu 965-8580, Japan 2004.

[41] Fonseca, Elza Maria Morais, Análise por Elementos Finitos do Comportamento de Tubagens sob a Acção de Fortes Gradientes Térmico. Dissertação para obtenção do Doutoramento em Engenharia Mecânica, Porto: FEUP - Faculdade de Engenharia da Universidade do Porto, 2003.

[42] Fonseca, E.M.M.; Vila Real, P.M.M., Finite element modelling of thermo-elastoplastic behaviour of hot-rolled steel profiles submitted to fire. In IV Congresso de Métodos Numéricos en Ingeniería. Sevilla, Espanha, 1999.

[43] ANSYS© Academic Research, Release 16.2, Help System, Element reference, ANSYS©, Inc.

[44] Djaafer Haddad, Belkacem Lamri, Elza MM Fonseca, Cellular Slabs With and Without Insulation Submitted to Fire Conditions, Actas das 5.as Jornadas de Segurança aos Incêndios Urbanos, Lisboa, LNEC, Portugal, 1 e 2 Junho 2016.